

A dark blue rectangular banner with a bokeh effect of light blue circles. The text "Imperial College London" is written in white, bold, sans-serif font on the left side.

Imperial College
London

Review of Distribution Network Security Standards

Extended Report Appendices

To the Energy Networks Association

March 2015

13 APPENDIX A – MODELLING

13.1 Overview

In this chapter a large array of modelling tools is presented in detail. In particular:

In Section 13.2 we present a basic overview of numerical approaches used in Monte Carlo reliability simulations. In particular, the use of Markov chains to model component failure and restoration is showcased along with suitable network searching methods suitable for computing Energy Not Served in complex distribution systems involving numerous assets and protection devices. Relevant reliability indices used throughout the report such as Expected Energy Not served (EENS), Customer Interruption (CI) etc. are also introduced. The section closes with an illustrative case study where a typical Monte Carlo reliability analysis is performed and the relevant metrics computed.

In section 13.3 we introduce the concept of chronological Monte Carlo reliability assessment. This approach utilises the principles illustrated in Section 13.2, but enables the accommodation of storage elements by modelling their chronological operation. Regarding the calculation of EENS for a given storage plant and network, a novel probabilistic calculation framework is proposed based on performing a large number of chronological simulations of the network equipped with the storage plant under investigation. Given that the storage plant's state-of-charge is coupled to preceding operating points and outage events, a chronological simulation of the system is necessary to compute EENS for a given scenario of transformer outages. Since these outages are random in nature with respect to their time of occurrence and the duration until they are restored, a probabilistic Monte Carlo framework sampling a large number of plausible events is required to infer the underlying system EENS. To alleviate the increased computational burden that this method may entail, an efficient bisection search algorithm is proposed to minimize the number of iterations performed until the Equivalent Load Carrying Capability value is computed.

In Section 13.4 a novel planning model is introduced enabling the balancing between investment costs and the impact of high impact low probability events. Risk-averseness to adverse faults is modelled via the spectral risk metric known as Condition Value-at-Risk (CVaR). The presented tool allows the planner to identify the most cost-efficient investment decisions in conventional line reinforcements and DSR schemes while ensuring that the operational cost arising due to adverse faults, which are being modelled in a probabilistic fashion on the basis of historical data, is bounded according to the planner's risk profile. This model constitutes a fundamental extension to the traditional cost-benefit planning framework, enabling the probabilistic consideration of faults in the interest of building more cost-efficient networks.

In Section 13.5 we introduce relevant reliability metrics employed in distribution network reliability analysis and outline the main idea of cost-benefit planning frameworks. We demonstrate how the optimal redundancy level that cost-efficiently balances cost of investment against the interruptions can be computed. This forms the basis of the current distribution planning philosophy and is expanded in the following sections.

In Section 13.6 we introduce a stochastic planning model, capable of minimizing expected investment cost across a scenario tree while allowing investment in transformers and DSR schemes. This type of modelling is helpful in cases where increased uncertainty characterises the long-term evolution of the distribution system. Examples of such cases include uncertainty surrounding long-term demand growth, penetration of distributed generation resources and/or electric vehicles etc. It is clear that such cases do arise in practice and a framework capable of identifying strategic actions to manage this uncertainty is required. The proposed model makes use of the inter-temporal resolution of uncertainty to identify the optimal investment strategy which encompasses cost-efficient contingent actions to cope with adverse scenario realisations. The adopted approach constitutes a necessary step beyond deterministic planning tools typically used and is bound to become increasingly relevant as distribution systems face increasing uncertainty and identifying cost-efficient flexibility-driven investments becomes an essential component of planning. This stochastic model is capable of quantifying the option value of DSR.

In Section 13.7 we introduce a stochastic planning model similar to section 13.6, but this time focusing on the operational flexibility made possible by investing in Soft Open Points (SOP). Modelling of this technology requires the consideration of reactive power flows. This model is particularly useful for planning in cases where voltage constraints are a concern. In particular, the large penetration of distributed generation (DG) sources can lead to voltage excursions beyond the network limits. The presented model can identify the optimal investment strategy incorporating re-conductoring with multiple conductor types and investment in SOPs to resolve the voltage rise problems when facing uncertainty regarding the long-term growth of DG. The full mathematical formulation is presented in detail and explained.

In Section 13.8 we present an alternative approach to dealing with long-term uncertainty. In contrast to sections 13.6 and 13.7 where the objective is the minimisation of expected cost across multiple scenarios, in this model the planner's objective is the minimisation of the maximum regret. This constitutes a highly risk-averse planning approach where scenarios are defined independent of probabilities and the planner's objective is the minimisation of regret experienced if the future was perfectly known. As in the stochastic case, the min-max model is capable of identifying attractive opportunities for strategic actions, recognising and valuing the flexibility embedded in smart grid assets such as DSR. The full mathematical formulation is presented with a focus on uncertainty on long-term demand growth.

In section 13.9 we analyse the impact that the DSR's capability to operate in islanding mode has on its security contribution. Various illustrative case studies are performed to demonstrate the impact of this capability in terms of two different reliability metrics; Equivalent Firm Capacity and Equivalent Load Carrying Capability.

Section 13.10 introduces the modelling framework that describes the operation of Dynamic Line Rating (DLR). DLR is a promising technology which can release latent network capacity through near-real-time consideration of the impact that environmental variables have on overhead lines' thermal ratings. Subsequently, an operation model is introduced capable of

modelling the operation of a network fitted with DLR. The model is capable of capturing the dependence between wind and thermal capacity increase which becomes extremely relevant in cases where the network has wind energy sources. Some example simulations are presented to demonstrate the model capabilities and the relevance of the different parameters considered.

In Section 13.11 showcases the modelling of Photovoltaic (PV) distributed resources. Different considerations such as the impact of cloud dispersion of PV output are discussed and their modelling is presented. In addition, the section showcases the way that a very large population of cloud conditions can be sampled and relevant reliability indices can be calculated within a Monte Carlo framework for the purpose of evaluating reliability performance of a system in the presence of large PV penetration.

Section 13.12 presents a probabilistic computation approach for computing relevant reliability indices in a system with different possible protection system outcomes.

In Section 13.13 presents a stochastic operational tool for the modelling of corrective actions. A quasi-steady-state approach has been adopted where different fault events are split in stages and the optimal control action at each time step is identified and engaged for the purpose of minimising demand curtailment across the system.

This work is further supplemented in Section 13.14 where a planning model capable of considering the aforementioned capability for corrective control. The planner is capable of investing in network assets, backup generation systems, corrective control as well as buy energy from the upstream grid. This model is suitable for identifying the optimal investment schedule across different assets enabling planners to identify opportunities for conventional reinforcement deferral through relying on post-fault actions and

Section 13.15 introduces an alternative to centralised network planning based on the fact that different customer types have different capability for load shifting and sensitivity to market prices. This is made possible through the large-scale rollout of smart meters where consumers are capable of communicating their individual preferences and flexibility. This information can be used by the planner to identify a more cost-efficient investment plan in order to maximise social welfare across its customer base. The full mathematical formulation for carrying out distribution planning in the presence of customers with different price elasticities and valuations of demand curtailment is presented.

13.2 Numerical approach using Monte Carlo Simulation

In order to calculate the cost of interruptions, a range of reliability techniques can be used. Two main approaches to evaluating security have been implemented in this study:

- Numerical approach based on Sequential Monte Carlo simulation
- Analytical approach based on Markov models, see section 13.5,

In some cases, the problems are too complex to be formulated and solved analytically and therefore require the application of numerical techniques to find the solutions, for instance in

cases of common-mode failures or if the problems involve time-dependent events. Monte-Carlo simulation is a widely used numerical technique in network reliability analysis.

Implemented Continuous Time Sequential Monte Carlo simulation approach is based on randomly generating asset faults and simulating supply interruption restoration and asset repair processes. The model can take into account overlapping faults i.e. an eventual other fault or faults during the repair of the original fault. In addition, asset maintenance is modelled with a possibility of other overlapping faults occurring during maintenance. Restoration process considers fault clearing, network reconfiguration for fault isolation and supply restoration, transfer capability of adjacent networks, use of alternative method of supply such as mobile generation and finally asset repair and return to service. Multiple years are modelled chronologically until a desired confidence level of accuracy is achieved. Model records parameters used for calculation of statistics, like probability and cumulative density functions as well as expected values of CI, CML, ENS, cost of interruption, repair and use of alternative supply options. The remaining part of this section describes the calculation of reliability indices and gives more details about modelling.

Reliability indices evaluation through sequential Monte Carlo simulation

Sequential Monte Carlo simulation is a method in which time-dependent system operation is simulated by sampling stochastic sequences and durations of system states. The system states are sampled according to the Markov model of each system component. By randomly sampling durations of component states, the stochastic sequence of system states can then be produced. The estimate of reliability indices for chronological system operation is computed as below:

$$\hat{E}(H) = \frac{1}{N} \sum_i^N H(X_i)$$

H is the estimation function of a reliability index such as Energy Not Supplied (ENS) or Customer Interruptions (CI). N is the number of simulated years, and X_i represents the chronological system state sequence and duration for year i .

Stochastic sampling of system state for a pre-set time period (here we use a year but other time horizons can be used if required) is described as follows:

- (1) Generate the initial state of each system component according to the probability distribution of their own Markov model.
- (2) Sample the transition time from the current state to the next possible state for each component. For those components that have multiple possible transitions, choose the state with the shortest transition time.
- (3) List and sort all component transition times in an ascending order. The set of all component states is the current system state and its duration is the shortest component transition time T_{min} . Set system simulation time as $T=T_{min}$.

- (4) Identify status for each node in the system and conduct power flow optimisation so that, at each load point, reliability indices can be computed for the current system state.
- (5) Deduct the shortest transition time from all component transition times and update the component state as the next sampled state. Sample a new transition time for the component with zero transition time for the new state.
- (6) Repeat step 3 and set system simulation time as $T=T+T_{min}$. Repeat step 4 to compute the reliability indices of the system state. If for a load point, the last status is “not supplied”, then increase the customer interruption counter by 1; otherwise, it is recognised as a continued interruption.
- (7) Repeat steps 3 to 6 until system simulation time T reaches the simulation horizon (one year). Evaluate and record the reliability indices of the system for this year.

The expected value and probability distribution of reliability indices can be evaluated by repeating the above procedure for N years. Convergence of the simulation is calculated using confidence intervals or coefficients of variation, which also serve as stopping criteria for the simulation.

As discussed before, the reliability indices used for measuring the DNOs performance in the UK are ENS, CI and CML (Customer Minute Lost). Time-sequential Monte Carlo simulation allows for calculating the real-time information of outages at each load point. An illustrative example of a load point outage can be seen in Figure 13.1. In this example, the sampled outage covers 3 system states with the critical time points at t_1 , t_2 , t_3 and t_4 , and system unserved power varying in time across P_1 , P_2 and P_3 .

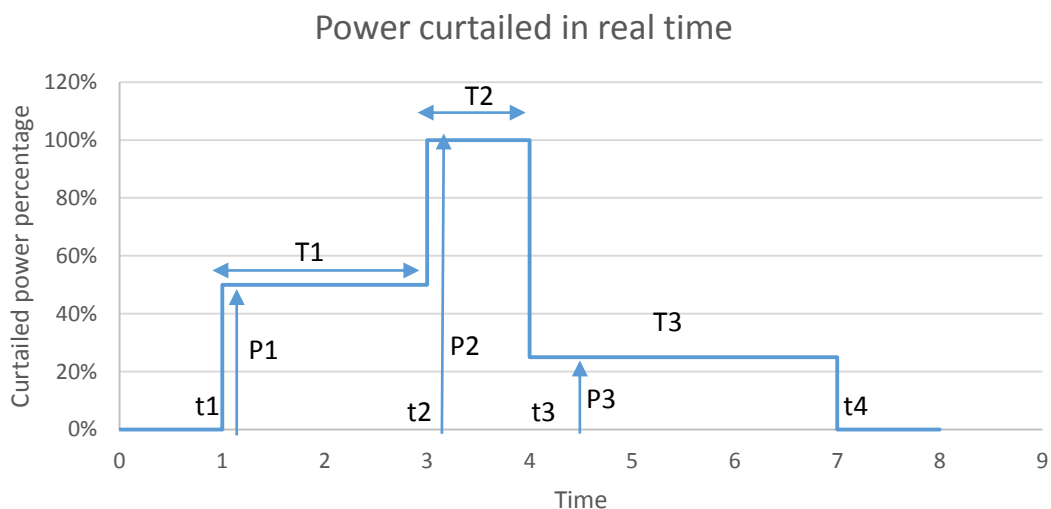


Figure 13.1: An illustrative example for load point outage in real time

The ENS for this outage is:

$$ENS = P_1 * (t_2 - t_1) + P_2 * (t_3 - t_2) + P_3 * (t_4 - t_3) = P_1 * T_1 + P_2 * T_2 + P_3 * T_3$$

The CML index for this load point is calculated as follows:

$$CML_i = \frac{P_1}{D_1} * N * T_1 + \frac{P_2}{D_2} * N * T_2 + \frac{P_3}{D_3} * N * T_3$$

Where D_i is the load point demand for the system state i and N is the number of customers at the load point.

System CML is adjusted as follows (note the multiplication by 60 to convert hourly values of CML_i to minutes):

$$CML_{system} = \frac{\sum_k CML_k}{\sum_k N_k} * 60$$

where k is the index of load point.

Finally, the CI index for the load point is found as:

$$CI_i = \max\left(\frac{P_1}{D_1}, \frac{P_2}{D_2}, \frac{P_3}{D_3}\right)$$

System CI is adjusted as follows (note the multiplication by 100 to convert the values per customer into the value per 100 customers):

$$CI_{system} = \frac{\sum_k CI_k}{\sum_k N_k} * 100$$

where k is the index of load point.

Node status in network operation

In the Monte Carlo simulation a graph representation is used where nodes represent network components and arcs logical linkages between nodes. Node status is a dynamic property of a node in network operation and is affected by its own node state as well as by the states of other nodes. Each node can be in one of three possible states:

- “Supplied” (Green): a supplied node means that the component at this node is not faulty and a live route from this node to a power source exists in which none of the nodes is isolated or interrupted.
- “Interrupted” (Red): an interrupted node represents that the component at this node is faulty but not yet isolated (fault clearing state) OR another node connected to this node is interrupted (affected by fault clearing). This status is usually found in a network where a fault happens and the associated feeder circuit breaker trips the branch so that other branches are protected. All nodes in this branch are interrupted and backup switching is not yet ready.
- “Isolated” (Black): an isolated node represents that the component at this node is faulty and is being repaired. It is internally isolated by opening the switchgear at the ends of the component. In this status, a backup switching action in network is available for previously interrupted nodes so that the open circuit breakers and normally open points can be closed if a live route to a power source exists.

A network searching method, *Depth-first technique*, is applied to the whole network for identifying the connectivity of each component in network.

The algorithm progresses through the network according to the following steps:

- (1) Tag all nodes as white (unchecked status)
- (2) Tag all nodes with components in “repair state” or “maintenance state” as black (isolated status)
- (3) Tag all nodes with components in “fault clearing state” as red (interrupted node)
- (4) From each interrupted node, iteratively search and tag every connected node as red (interrupted) unless it is already black (isolated) or the component associated with that node is a circuit breaker or NOP
- (5) From each node with a power source, iteratively search and tag every connected node as green (supplied) unless it is black (isolated) or red (interrupted)

After the above steps are completed, the status of all components can be identified except for those tagged as white (unchecked), which are regarded as unsupplied nodes.

Power flow optimisation

In distribution network planning and operation the rated capacities of lines, circuit breakers and transformers need to be carefully considered. When there is a fault, switching actions may occur to restore the supply to interrupted customers through other sources. In this situation however the capacity constraints of system components may limit the system restoration ability. Therefore, an optimisation algorithm is applied in our model to minimise the energy not served while considering all component constraints. The input parameters for load flow calculations are as follows:

- Available distributed generation at node i : G_i
- Load level at node i : L_i
- Power flow from node i to node j : $f_{link_{ij}}$
- Connectivity between node i and node j : $\pi_{link_{ij}}$

Objective function:

$$Min f = Min \{ \sum Load_{curtailment_i} \}$$

Constraints:

$$0 \leq G_i \leq G_{i_{max}}$$

$$-f_{link_{ij_{max}}} \leq f_{link_{ij}} \leq f_{link_{ij_{max}}}$$

$$G_i + Load_{curtailment_i} - \sum \{ \pi_{link_{ij}} \cdot f_{link_{ij}} \} = L_i$$

For isolated and interrupted nodes, the flow limits of the connected arcs/links are set to zero.

Network component modelling

This section discusses the modelling of network components to enable modelling of node states using Markov processes. Colour tagging and Depth-first network searching algorithm are then applied in node status identification to simulate system failure restoration.

The model allows for selecting which component can fail (while for the others it is assumed that no failure can occur), as well as considering different failure modes including short circuit failure, open circuit failure and failure to respond when supposed to.

When a component fails, the simulation proceeds through the following steps:

Identify failure location

Determine the switching of the corresponding circuit breakers to isolate the fault area

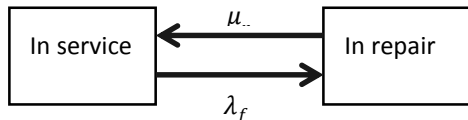
Restore as many load points as possible when backup is available

Restore supply when repair is complete

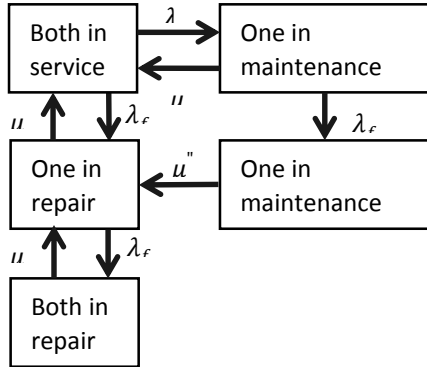
In the following we describe how different network components are modelled in Monte Carlo simulations. The status of a network component is modelled as a Markov process. Four general component states are used to represent the component operational status:

- “Up state”: the component is working correctly;
- “Fault clearing state”: the component is faulty; the fault has been cleared by opening the corresponding feeder circuit breaker, but the switching action to isolate the fault for restoration is not yet ready;
- “Repair state”: switching action has been taken to isolate the component for repairing, interrupted load points are resupplied if possible;
- “Maintenance state”: the component is undergoing scheduled maintenance and is disconnected.

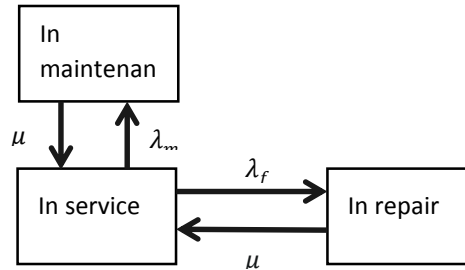
Figure 13.2 illustrate four Markov models for transformer and lines. They are used for representing distribution transformers, primary and bulk supply substations, and lines and cables.



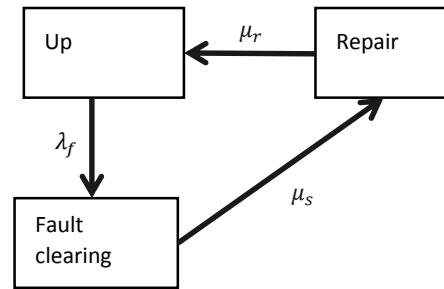
Distribution transformer with circuit breaker



Two parallel transformers



Transformer with maintenance



Line with switchgear

Figure 13.2: Illustration of four Markov models for transformers and lines

Illustrative case studies

In order to illustrate the use of analytical and numerical techniques in reliability analysis, a range of studies has been carried out on a typical radial HV distribution network, as shown in Figure 13.3. The HV network is connected to an EHV network through a primary substation which is composed of busbars, two 33/11 kV transformers and circuit breakers (CB). At the 11 kV level, the substation is connected to feeders where a protection circuit breaker is installed. When there is a short circuit failure in lines or cables, the corresponding CB will trip the downstream branch instantly without interrupting upstream or other branches.

The 11 kV network is configured as a radial network with a normally open circuit breaker that connects adjacent branches for back-feeding during an outage. All network sections are equipped with normally closed switchgears at one or both sides. When a failure is identified, the switching action will isolate the failed section by opening the corresponding switchgears and the affected load points can be resupplied through the adjacent branch. At each load point, an 11/0.4 kV transformer is connected through a circuit breaker or fuse, which will disconnect the load point if the LV transformer fails, not affecting the rest of the network.

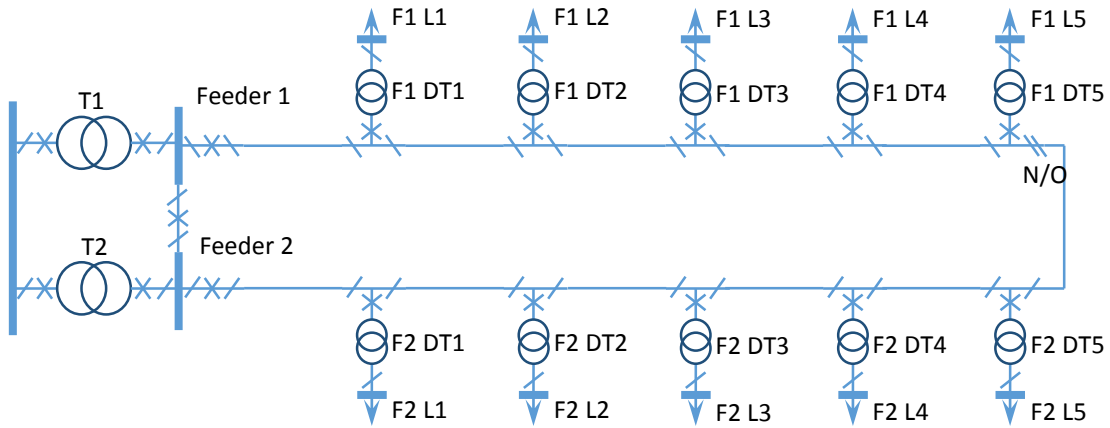


Figure 13.3: An example of radial HV distribution network

In our reliability assessment model the network is represented as shown in Figure 13.4, where nodes in the graph represent system components: EHV feeder, circuit breakers, 33/11 kV transformers, lines with sectionalising switches, NOPs, LV transformers with circuit breakers and load points. Arcs represent logic linkages between the elements of the network.

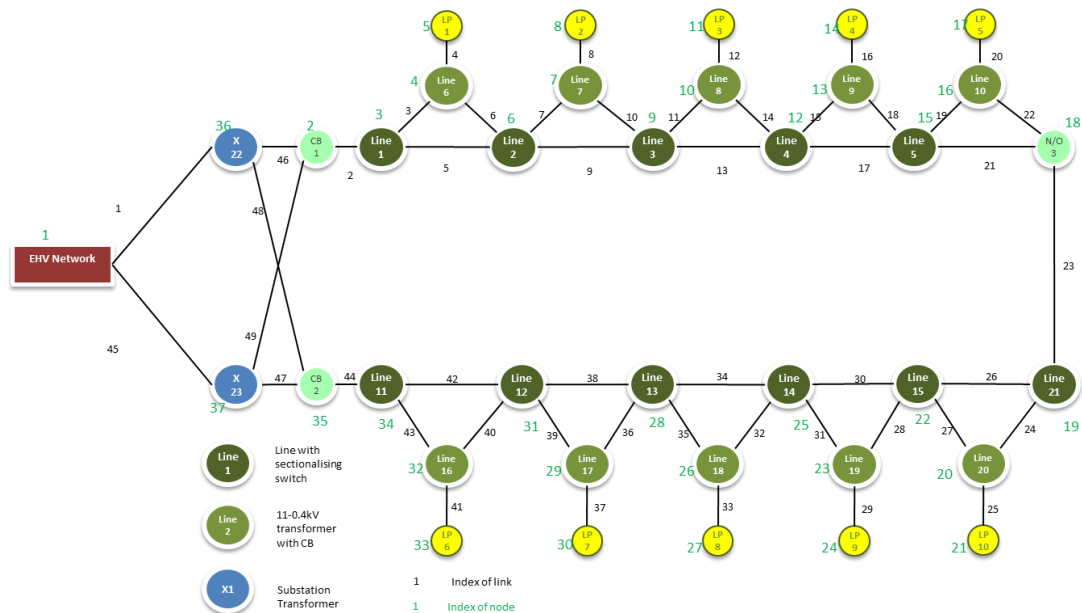


Figure 13.4: Graph representation of HV network for reliability assessment

The proposed method is used to obtain probability distributions of network reliability indices. A case study is presented here in which the assumed line section length is 0.25 km, network feeder capacity conforms to the N-1 criterion, no emergency generation is available for load points, and 30 minutes is the assumed duration of manual network switching.

Figure 13.5 shows the PDF (probability distribution function) bars and CDF (cumulative distribution function) curves for ENS for line failure rates of 2%, 5%, 10% and 20% per km and year. Depicted range of ENS values is between 0 and 10 MWh/year.

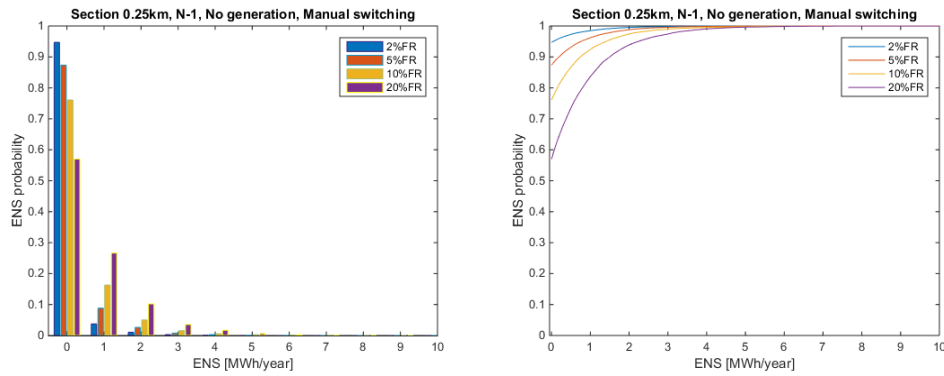


Figure 13.5: PDF and CDF of ENS for failure rate of 2%, 5%, 10% and 20%/km.year

The results suggest that the probability of annual ENS being zero is up to 95% for low failure rates (associated with underground cables), while it is about 57% for high failure rates (more common for overhead lines). The PDF bars in Figure 13.5 follow an exponential distribution. It can further be seen from the CDF chart that there is a 95% likelihood that ENS is lower than 0.1 MWh/year for the failure rate of 2%, 0.8 MWh/year for 5%, 1.4 MWh/year for 10% and 2.2 MWh/year for 20% failure rate.

Figure 13.6 shows PDF bars and CDF curves for CI for network failure rates of 2%, 5%, 10% and 20% per km and year, with CI ranging between 0 and 250 occ./100customer/year.

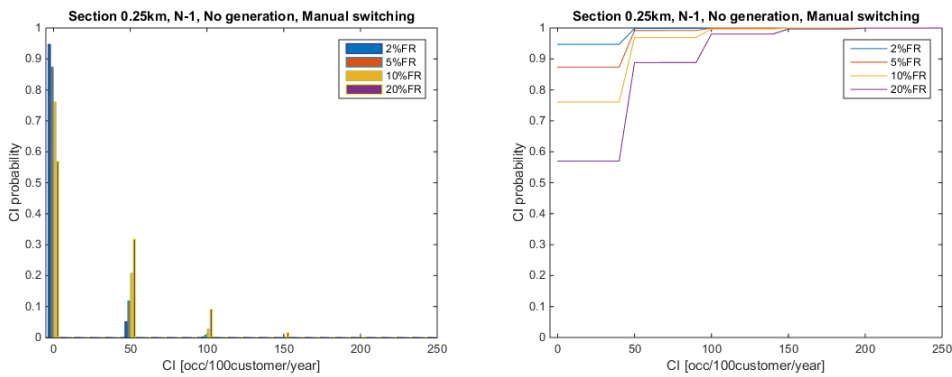


Figure 13.6: PDF and CDF of CI for failure rate of 2%, 5%, 10%, 20%/km.year

The probability of annual CI being 50 occ./100customer.year is around 5% for low failure rates, but is as high as 32% for high failure rates. The PDFs again suggest an exponential distribution. The CDF chart suggests that the probability of CI index being 50 occ./100customer.year or below is 99.9% for failure rate of 2%, 99.2% for 5%, 96.9% for 10% and 88.8% for 20%.

Figure 13.7 shows the PDF bars and CDF curves for the CML index, again looking at failure rates of 2%, 5%, 10% and 20% per km and year.

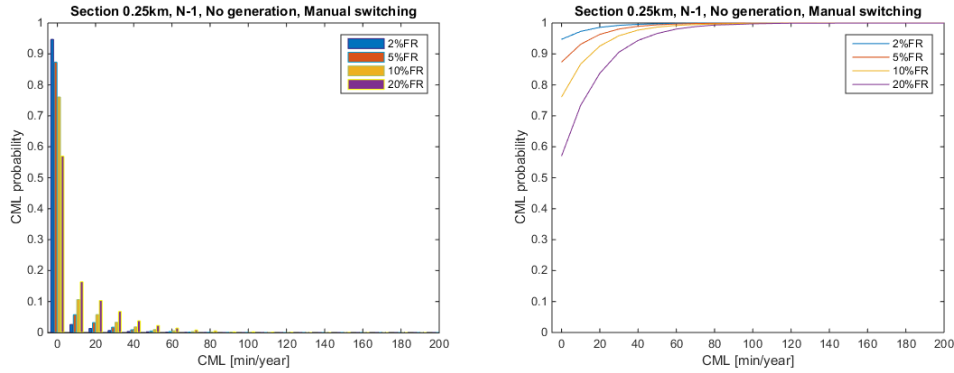


Figure 13.7: PDF of CML for failure rate of 2%, 5%, 10%, 20%/km.year

According to the results, the probability of annual CML being at the level of 10 min/customer.year is about 2% for low failure rates and about 16% for high failure rates. The CDF curves further suggest that the probability of CML being at or below 20 occ./customer.year is 98.6% for 2% failure rate, 96.3% for 5%, 92.5% for 10% and 83.7% for 20%.

Expected ENS, CI and CML

A set of further case studies has been carried out for different values of input parameters shown in Table 13.1.

Table 13.1: Case studies parameters

Parameter	Values
Failure rate for overhead lines (%/km.year)	5 and 20
Failure rate for underground cables (%/km.year)	2 and 10
Switching time (minutes)	2 (automatic) and 30 (manual)
Restoration time (hours)	3 (mobile generation) and 24 (repair)
Section length (km)	0.25 and 1
Loading level	N-1 and N-0

Table 13.2 shows the resulting expected values of ENS for different HV network reliability parameters, switching times and loading levels.

Table 13.2: EENS for different HV network reliability parameters, switching time and loading level

Network ENS (MWh/year)	Failure Rate (%/km.year)	Automatic switching				Manual switching			
		MTTR 3h		MTTR 24h		MTTR 3h		MTTR 24h	
		N-1	N-0	N-1	N-0	N-1	N-0	N-1	N-0
Section length 0.25 km	2%	0.00	0.10	0.00	0.71	0.04	0.17	0.04	0.84
	5%	0.01	0.25	0.01	1.85	0.10	0.40	0.11	1.93
	10%	0.02	0.53	0.02	3.71	0.22	0.85	0.22	4.21
	20%	0.03	0.97	0.04	7.69	0.43	1.66	0.45	8.52
Section length 1 km	2%	0.01	0.40	0.01	2.87	0.17	0.68	0.17	3.24
	5%	0.03	1.07	0.04	7.51	0.46	1.68	0.45	8.22
	10%	0.07	2.03	0.11	15.16	0.90	3.35	0.88	16.86
	20%	0.15	4.03	0.31	29.97	1.74	7.29	1.95	35.84

Table 13.3 shows the results for the expected values of CI for different HV network reliability parameters, switching times and loading levels.

Table 13.3: ECI for different HV network reliability parameters, switching time and loading level

Network ECI (occ./100 cust.year)	Failure Rate (%/km.year)	Automatic switching				Manual switching			
		MTTR 3h		MTTR 24h		MTTR 3h		MTTR 24h	
		N-1	N-0	N-1	N-0	N-1	N-0	N-1	N-0
Section length 0.25 km	2%	3	3	3	4	3	3	3	4
	5%	7	8	7	10	7	8	7	9
	10%	14	15	14	19	14	15	14	20
	20%	27	29	27	39	27	30	28	41
Section length 1 km	2%	11	12	11	15	11	12	11	15
	5%	29	31	27	38	31	30	28	40
	10%	54	59	55	78	57	58	55	79
	20%	109	124	110	156	110	128	111	166

Finally, Table 13.4 shows the expected values of CML for different HV network reliability parameters, switching times and loading levels.

Table 13.4: ECML for different HV network reliability parameters, switching time and loading level

Network ECML (min/customer.y ear)	Failure Rate (%/km.year)	Automatic switching				Manual switching			
		MTTR 3h		MTTR 24h		MTTR 3h		MTTR 24h	
		N-1	N-0	N-1	N-0	N-1	N-0	N-1	N-0
Section length 0.25 km	2%	0	1	0	6	1	1	1	7
	5%	0	2	0	14	2	3	2	15
	10%	0	4	0	29	4	7	4	34
	20%	1	8	1	61	8	15	9	69
Section length 1 km	2%	0	3	0	23	3	6	3	26
	5%	1	8	1	59	9	15	9	66
	10%	1	16	2	119	17	29	17	136
	20%	3	32	6	237	33	64	37	290

Comparison between sequential Monte Carlo simulation and analytical method

Differences between results obtained using sequential Monte Carlo simulation and the analytical method applied to the same network are presented in Table 13.5.

Table 13.5: Difference of EENS obtained by Monte Carlo simulation and by analytical method

Network ENS (MWh/year)	Failure Rate	Automatic switching				Manual switching			
		MTTR 3h		MTTR 24h		MTTR 3h		MTTR 24h	
		N-1	N-0	N-1	N-0	N-1	N-0	N-1	N-0
Section length 0.25 km	2%	-4.1%	-4.9%	-2.8%	-8.5%	-7.2%	-3.6%	-0.1%	-0.3%
	5%	-2.8%	-1.2%	-0.2%	-3.9%	-4.1%	-8.7%	-0.4%	-8.7%
	10%	5.3%	5.0%	-10.5%	-3.8%	-0.1%	-3.1%	-0.1%	-0.4%
	20%	-5.9%	-4.6%	2.4%	-0.5%	-1.5%	-4.7%	2.4%	0.7%
	2%	2.0%	-2.1%	0.1%	-6.9%	-0.9%	-1.9%	-1.4%	-4.1%

Network ENS (MWh/year)	Failure Rate	Automatic switching				Manual switching			
		MTTR 3h		MTTR 24h		MTTR 3h		MTTR 24h	
		N-1	N-0	N-1	N-0	N-1	N-0	N-1	N-0
Section length 1 km	5%	0.4%	5.3%	11.0%	-2.8%	6.6%	-3.9%	2.4%	-2.8%
	10%	5.3%	0.3%	9.7%	-2.0%	4.1%	-4.1%	-3.1%	-0.5%
	20%	7.1%	-0.7%	5.3%	-3.4%	0.3%	4.3%	3.0%	5.5%

The simulation stopping criteria for all case studies in the sequential Monte Carlo simulation was when a Coefficient of Variation (CoV) of 5% or less was achieved. According to the statistical theory, the simulation error greater than two standard deviations occurs with less than 5% probability. Thus, in this distribution network reliability study, the probability of simulation error greater than 10% of the actual value is about 5%. From Table 13.5, there are 2 cases (out of 64) with errors greater than 10%. This corresponds to 3% of cases being beyond the (-10%, +10%) interval, which is within the adopted range for CoV of 5%.

13.3 Storage modelling via chronological Monte Carlo simulation

The central step in calculating the contribution of a particular asset to security of supply is to compute the system's EENS when equipped with the asset under investigation and compare with the EENS in the absence of the asset. An important issue is that energy storage devices have "state memory" as the state of charge is coupled to the preceding operational decisions. Whereas DG is solely constrained by its technical and resource availability (e.g. fuel, wind etc.) and maximum stable generation level, the storage facility must have both enough power output capability and energy stored to supply the load. In other words, whereas conventional resources, such as DG, typically face only power constraints, storage facilities can face both power and energy constraints. These constraints can be independent or combined. For example, it is possible to have sufficient amount of energy stored but the maximum storage output may be less than the peak demand to be served; a power constraint arises. The opposite situation of an empty tank and sufficient power capability gives rise to an energy constraint. Naturally, there may also be cases where there is insufficient energy in the tank and the plant's power output capability is less than the demand to be served; this is a case of a combined power and energy constraint occurrence. As a consequence of the above, the actual shape of the demand peak being served is important in addition to the peak magnitude. As a result, whereas DG contribution can be estimated using load-duration-curve-based methods, *chronological* modelling of the operation of the storage facility is essential to identify occurrences of power and energy constraints and quantify the unsupplied energy. Carrying out chronological analysis where the storage plant is operated along the time horizon under study is necessary to identify cases of energy and/or power constraints.

In sequential Monte Carlo simulation, chronological system histories are synthesized by combining randomly-generated outage events with hourly chronological loads. Consequently, the system can be modelled in great detail with an accurate representation of outage duration

which is particularly important in the case of storage operation. The use of Monte Carlo simulation allows for the calculation of probability distribution of all state variables and ultimately the computation of EENS for a particular distribution system. The main equations involved in simulating a system with storage are shown below, along with the corresponding nomenclature.

Nomenclature

D_t	Residual demand above the network transfer limit at hour t (MW)
ε	Storage device energy efficiency (scalar between 0 and 1)
E_t	Stored energy at the end of hour t (MWh)
E_0	Initial state-of-charge (MWh)
P_t	Power discharged/charged by storage device at hour t (MW)
U_t	Unsupplied energy at hour t (MW)
E^{max}	Maximum energy capability of storage plant (MWh)
P^{max}	Maximum power capability of storage plant (MWh)
C_t	Network capacity at hour t (MW)

Mathematical Formulation

$$ENS = \sum_{\forall t} U_t \quad (3.1)$$

$$E_t = \min(E^{max}, E_{t-1} + \varepsilon \min(P^{max}, C_t - D_t)), \text{ if } D_t \leq C_t \quad (3.2)$$

$$E_t = \min(E^{max}, E_{t-1} + \min(P^{max}, C_t - D_t)), \text{ if } D_t > C_t \quad (3.3)$$

$$P_t = E_t - E_{t-1} \quad (3.4)$$

$$U_t = D_t - C_t - P_t \quad (3.5)$$

The above formulation enables the computation of ENS. In particular, equation (3.2) holds when demand is below the network's capacity limit and simulates the storage plant's charging action. Note that the charging rate is capped at the plant's charging limit and the state-of-charge cannot surpass the plant's energy capacity limit. Also, note that in (3.2) the impact of energy efficiency has been considered; some amount of charging energy is lost. Conversely, equation (3.3) governs storage discharging which occurs in cases where the demand to be served exceeds the currently-available network capacity. Equation (3.4) computes the power output of the storage plant as the difference between two consecutive states of charge; positive P_t denotes charging power, while negative denotes discharging. Finally, equation (3.5) calculates the amount of curtailed demand as the difference between residual demand to be served and discharged power. Finally, Energy Not Served is calculated as the overall sum of unserved energy across the simulation duration, as shown in (3.1).

Modelling asset availability

In general, EENS is derived using a probabilistic calculation, in recognition of the stochastic availability of network assets. This probabilistic analysis should not only reflect the average availability of each component, but also the duration of each outage. Outage duration modelling is extremely important to be modelled in order to accurately capture the energy constraints that result from prolonged outages. We are interested in modelling the reliability of transformers. In general, a transformer's technical availability depends on two metrics:

Mean Time Between Failures (MTBF) – expressed in hours

Mean Time to Restore/Repair (MTTR) – expressed in hours.

ELCC calculation

Having computed the EENS for the basecase without storage, the calculation of ELCC of a particular storage plant is essentially a root-finding problem of solving the equation:

$$EENS^* - EENS(D + ELCC) = 0 \quad (3.6)$$

where D is the basecase peak demand level and $EENS^*$ denotes the basecase supply risk level. Several search methods exist to solve this problem; in our case the bisection root-finding method is employed to calculate ELCC. In brief, the bisection method repeatedly bisects a given search interval (in this case, it can be defined as $[D, D + \gamma P^{max}]$, where $\gamma > 1$ given that ELCC can in certain cases be above 100% of the storage plant's power capability) and selects the sub-interval in which the root must lie, continuously refining the search domain until a close match is found and the stopping criterion of the form $(EENS^* - EENS(D + ELCC))^2 < \varepsilon$ for small ε is met.

Example simulations of storage operation

In this section we will briefly demonstrate the main working principles of the proposed ELCC calculation framework. As already stated, ELCC computation involves the calculation of ENS across many thousands of transformer outage scenarios, sampled from exponential distributions with the specified Mean Time Between Failures (MTBF) and Mean Time to Repair (MTTR).

In Figure 13.8 we present operation of a storage plant of power rating 2 MW and 20 MWh energy capacity (denoted 2 MW/10 hours) across a sampled year. The system consists of two 10 MW transformers, each with MTBF of 1 year and MTTR of 240 hours. In the figure below we plot the demand time series (MW), the network status (intact, N-1 or N-2), the storage status (plant assumed to be perfectly reliable in this case), the storage power (MW) where positive values correspond to charging and negative values to discharging events, state-of-charge (SOC) in MWh and unserved power in the bottom (MW). Peak demand is set at 13 MW i.e. above the network N-1 limit.

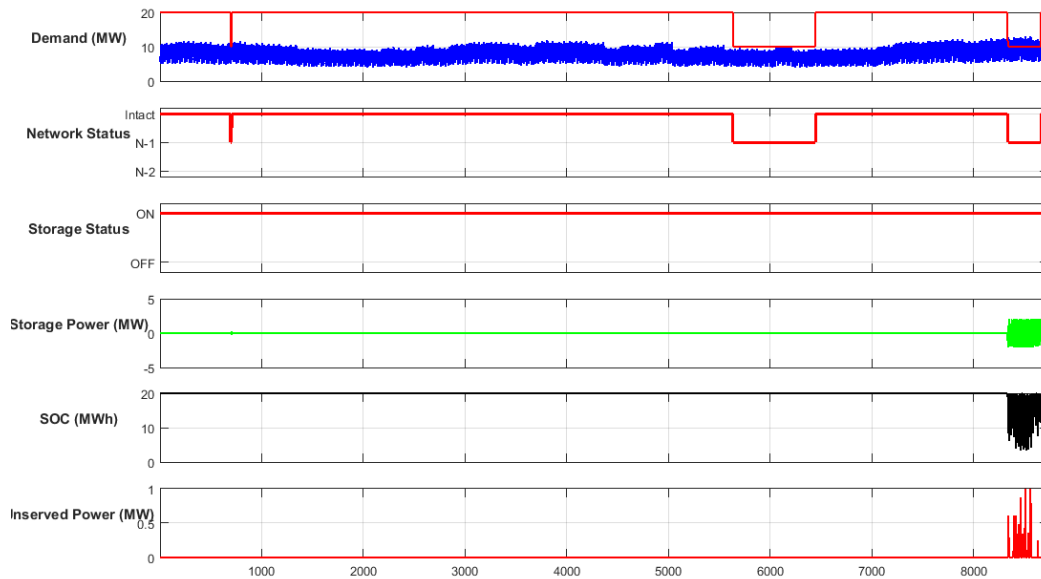


Figure 13.8: Storage operation for a sample year. MTBF = 1 year, MTTR = 240 hours. Storage size is 2 MW/10 hours.

As can be seen above, there is a total of 3 single outages occurring throughout the simulated year. In the first two cases, single outages occur in a part of the year that demand is relatively low. As a result, there is no need to engage the storage plant for supply support. However, the last fault occurs during December which experiences high demand. As a result, the storage plant is engaged, as evidenced by the fluctuating power (green curve) and SOC (black curve). At the same time, some unserved power arises due to power constraint that the storage plant is facing; peak residual demand to be served during this period is as high as 3 MW, whereas the plant's power rating is only 2MW. This is also indicated by the fact that the SOC never reaches 0, i.e. although there is stored energy it cannot be supplied due to the maximum power rating being reached. The main principle of ES security contribution in this case is the periodic charging during night-time hours and subsequent discharging during high-demand afternoon hours. For this particular simulation, ENS = 208 MWh.

In Figure 13.9 we show operation of the same storage plant for a different sampled year. In this case, there are more failures being sampled, including a double outage event. As can be seen below, although the single outages occur at times when no demand curtailment arises due to low electricity consumption levels, the double outage event inadvertently lead to high ENS. In particular, during the double outage the storage is incapable of accessing the upstream network. As a result, once the initially-stored energy is depleted, the storage plant can no longer support security of supply, resulting in very high demand curtailment levels. This is exacerbated by the long repair time of transformers; in this particular sampled realisation, the double outage is repaired within 200 hours. Overall ENS in this case surpasses 2000 MWh. However, it is imperative to note that double outages are comparatively rare events and only very few sampled scenarios will result in such high ENS figures.

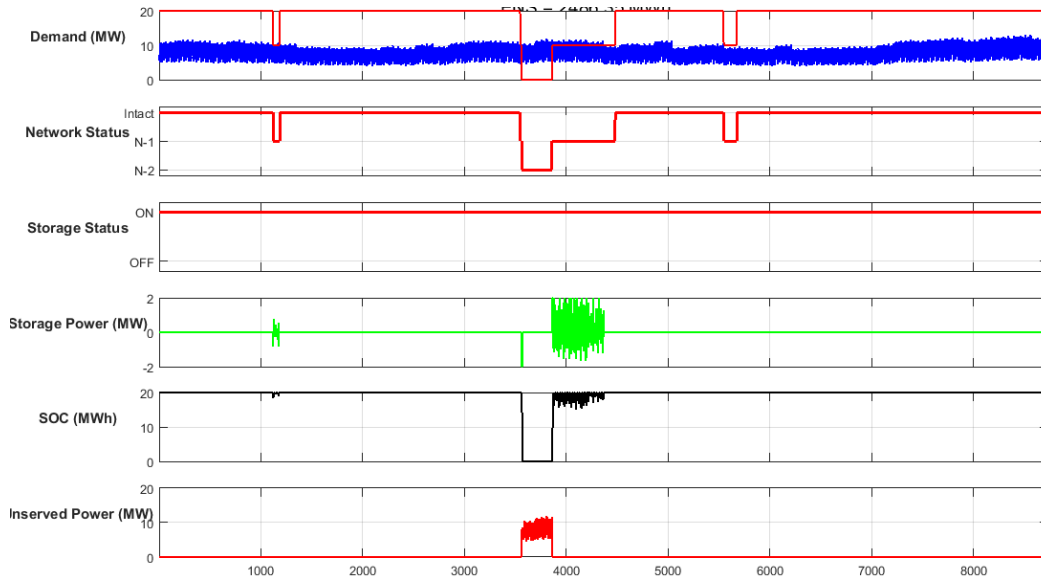


Figure 13.9: Storage operation for a sample year. MTBF = 1 year, MTTR = 240 hours. Storage size is 2 MW/10 hours.

A general fact to note is that although we present annual simulations above, in practice all Monte Carlo realisations are simulated chronologically one after the other. This is required to ensure that the effect of the initial state-of-charge E_0 choice is minimal. Operation has been split here in specific years just for the purpose of easy visualisation.

Monte Carlo ELCC calculation

Exploring the convergence behaviour of EENS calculation is a step of paramount importance to ensure that the calculated security contribution is satisfyingly close to the true underlying value. For this purpose, convergence behaviour analysis is undertaken to determine the number of Monte Carlo simulations to be performed. Naturally, the variability of the stochastic process as well as the relation between the stochastic process and EENS largely drive convergence behaviour. As an example, we show EENS convergence behaviour for the case where MTBF = 1 year and MTTR = 240 hours and a 2MW/10 hours storage plant is connected to the system. As can be seen in Figure 13.10, a few thousands Monte Carlo runs are required to reach convergence. It is clear that at 10,000 runs steady state behaviour has been reached at 38.1 MW. However, it is important to note that the particular case simulated here exhibits faster convergence compared to scenarios where transformer failures occur more rarely. For this reason, we have decided to simulate 1 million Monte Carlo runs throughout to guarantee good approximation of EENS. A very fast simulation algorithm has been developed and deployed to enable the simulation of a million years of storage operation without running into time and memory constraints.

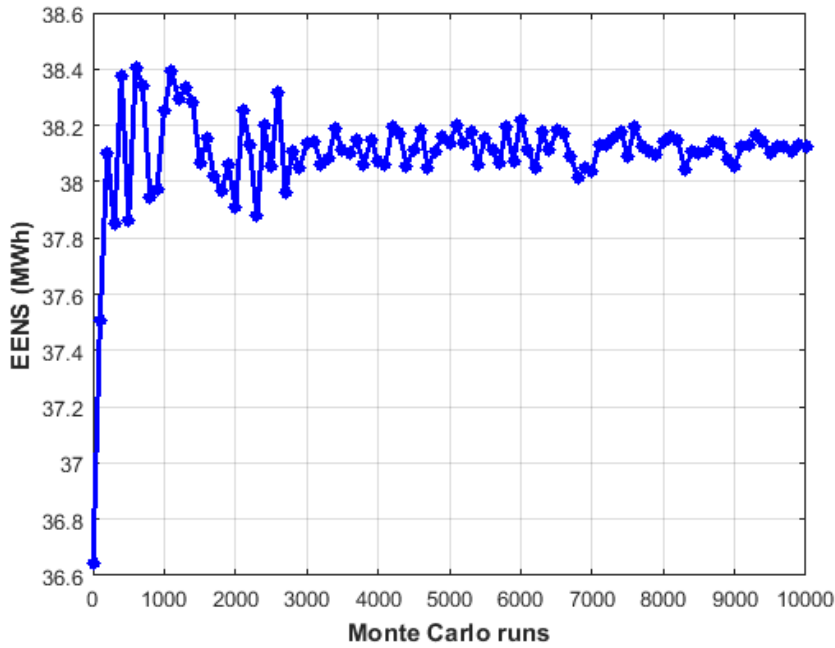


Figure 13.10: Example Monte Carlo convergence in the calculation of EENS.

In Figure 13.11 we show the convergence behaviour of the bisection root-finding method employed to identify ELCC in the case of MTBF = 1 year and MTTR = 240 hours. As shown in the plot below, seven iterations are required to reach the target EENS of 38.2 MWh. The search starts from an ELCC of 5MW, heuristically defined as the midpoint of the basecase secure transfer limit, and successive refinements are made until the ELCC value at which the basecase EENS can be reached is identified. The final computed ELCC for the 2MW/10h storage plant is 0.15 MW.

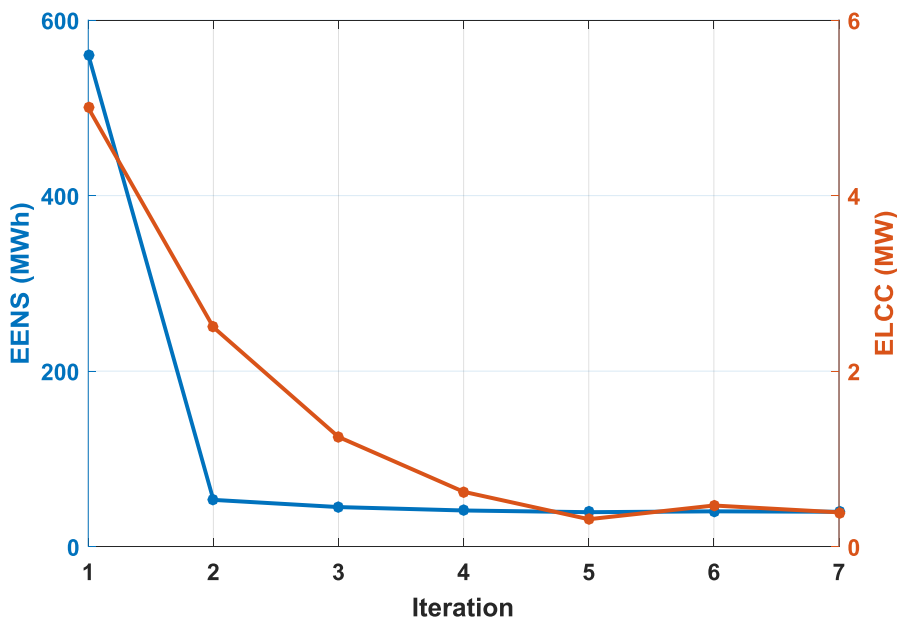


Figure 13.11: Example convergence of the bisection root-finding method to compute ELCC.

13.4 Non-network technologies portfolios to increase robustness of distribution networks against high impact low probability events caused by natural hazards: A CVaR optimisation approach

CVaR model's mathematical formulation

The presented model minimises the overall cost of investment in transformers and transfer cables that can be used to import/export power from/to neighbouring substations, along with the availability costs of DSR and backup generation's fuel cost (which may include a rental fee). We first introduce the model nomenclature follows by the objective function and constraints.

Nomenclature

Input Parameters

\bar{C}	Standardised size of each transfer cable	[MW]
$CVaR$	Conditional Value at Risk upper bound	[MWh/h]
Dem_t	Demand in period t	[MW]
\bar{G}	Maximum backup generation capacity	[MW]
$VoLL$	Value of lost load	[£/MW/yr]
α	CVaR confidence level	[p.u.]
γ	Number of DSR facilities	
δ	Total number of hours	[h]
δ_t	Number of hours in period t	[h]
π^{Ck}	Investment cost of cable k	[£/yr]
π^{DSR}	DSR utilisation fee	[£/MWh]
$\pi^{\overline{DSR}}$	DSR availability fee	[£/MW/h]
π^G	Fuel cost (and rental fee) of backup generating units	[£/MWh]
π^T	Investment cost of transformer	[£/MW/yr]
ρ_s	Probability of outage state s	[p.u.]
τ	Number of transformers	
φ_s^{Ck}	Availability factor of cable k in outage state s (0 if outaged, 1 if available)	
$\varphi_s^{\overline{DSR}i}$	Availability factor of DSR facility i in outage state s (0 if outaged, 1 if available)	
φ_s^{Tj}	Availability factor of transformer j in outage state s (0 if outaged, 1 if available)	

Decision Variables

$a_{t,s}$	Demand shed in period t and outage state s above levels defined by Value at Risk threshold	[MW]
C_k	Binary variable associated with construction of transfer cables (1 if cable k is built)	1/0
$DSR_{t,s}$	Total demand side response exercised at period t in outage s (through all DSR facilities)	[MW]
\overline{DSR}	Demand side response contracted and available in every period in each facility (there are γ DSR facilities)	[MW]
$G_{t,s}$	Production of backup generation in time t and state s	[MW]
$PNS_{t,s}$	Power not supplied in period t during outage s	[MW]
X_s	Substation capacity available during outage s (considering no contribution from DSR facilities)	[MW]
X_s^{DSR}	Substation capacity available during outage s (considering contribution from DSR facilities)	[MW]
T	Capacity of each transformer (there are τ transformers)	[MW]
z	Value at risk (VaR)	[MWh/h]

Sets

Nc	Number of substation components
Ns	Set of outage states (considering intact system)

Nt Set of time periods
 Nk Set of candidate cables

If the substation capacity, backup generation and DSR do not suffice to cover demand in a particular scenario (i.e. an operating condition under a given outage), demand is curtailed at a cost equal to the value of lost load (VoLL) and this is shown in Eq. (4.1) (where $ENS_{t,s} = \delta_t PNS_{t,s}$). Outage probabilities ρ_s (of each outage state $Ns=2^{Nc}$, where Nc is the number of substation components) are calculated by using forced outage rates (FOR) of substation components which, in turn, are obtained from outage and repair rates.

$$\begin{aligned} \text{Min}_{\substack{T, C_k, \overline{DSR} \\ DSR_{t,s}, PNS_{t,s} \\ G_{t,s}, X_s, X_s^{DSR} \\ a_{t,s}, z}} \left\{ \tau \pi^T T + \sum_{k \in Nk} \pi^{C_k} C_k + \gamma \delta \pi^{\overline{DSR}} \overline{DSR} + \sum_{t \in Nt, s \in Ns} \delta_t \rho_s \pi^{DSR} DSR_{t,s} \right. \\ \left. + \sum_{t \in Nt, s \in Ns} \delta_t \rho_s \pi^G G_{t,s} + \sum_{t \in Nt, s \in Ns} \delta_t \rho_s VoLL PNS_{t,s} \right\} \quad (4.1) \end{aligned}$$

Eq. (4.2) shows that substation capacity (X_s) changes in every outage state according to binary parameters φ that represent whether a given substation equipment is outaged ($\varphi = 0$) or available ($\varphi = 1$). Eq. (4.3) considers the contribution from DSR and backup generating unit to substation capacity (as backup generation is used only under outage conditions, we consider high reliability levels associated and that all units' contributions can be aggregated in a single generator).

$$X_s = \sum_{j \in 1..\tau} \varphi_s^T T^j + \sum_{k \in Nk} \varphi_s^{C_k} C_k \bar{C} \quad \forall s \quad (4.2)$$

$$X_s^{DSR\&G} = X_s + \sum_{i=1..\gamma} \varphi_s^{\overline{DSR}_i} \overline{DSR}_i + \varphi_s^G \bar{G} \quad \forall s \quad (4.3)$$

The part of demand that cannot be covered through “firm” substation capacity, backup generation and DSR, has to be ultimately curtailed and this is shown in Eq. (4.4). DSR cannot be exercised beyond the contracted amount and this is shown in Eq. (4.5). Likewise, backup generation also presents an upper limit as shown by Eq. (4.6), which should represent volumes of demand that can be realistically covered through backup generating units (e.g. 10% of peak demand).

$$X_s + DSR_{t,s} + G_{t,s} + PNS_{t,s} \geq Dem_t \quad \forall t, s \quad (4.4)$$

$$DSR_{t,s} \leq \sum_{i=1..y} \varphi_s^{\overline{DSR}_i} \overline{DSR} \quad \forall t,s \quad (4.5)$$

$$G_{t,s} \leq \varphi_s^G \bar{G} \quad \forall t,s \quad (4.6)$$

Transfer cables are built not only to import power from neighbouring substations, but also to export and support neighbouring substations if needed, and therefore capacity of transformers has to suffice and thus supply the peak demand and exports through transfer cables, which is shown in Eq. (4.7).

$$\tau T \geq \max\{Dem_t\} + \sum_{k \in Nk} C_k \bar{C} \quad (4.7)$$

To constrain risk exposure to HILP events, we use linear representation of CVaR as shown in Eq. (4.8) and (4.9).

$$PNS_{t,s} - z \leq a_{t,s} \quad \forall t,s \quad (4.8)$$

$$z + \frac{1}{1-\alpha} \sum_{t \in Nt, s \in Ns} \frac{\delta_t \rho_s}{\delta} a_{t,s} \leq CVaR \quad (4.9)$$

We use extremely small values of $1-\alpha$ in order to fully limit the impacts of events that are extremely rare (e.g. outage of multiple components such as transformers together with DSR facilities). Hence $1-\alpha$ is chosen after analysing the probability density function (PDF) of ENS associated with a solution where Eq. (4.9) is not imposed (i.e. risk-neutral solution) and thus $1-\alpha$ is set so as to capture impacts of extreme events only which are located at the right “tail” of the PDF. All variables in Eq. (4.1)-(4.9) are continuous and positive except for C_k that are binary, and the model has been implemented in FICO Xpress.

13.5 Analytical approaches for reliability evaluation

The main objective of reliability evaluation of distribution networks is to determine the values of reliability indices that measure the performance of the system in question. In this report, the following reliability performance indices are used: Energy Not Supplied (ENS), frequency of interruptions i.e. Customer Interruptions (CIs) and duration of interruptions i.e. Customer Minutes Lost (CML), as well as the reliability worth indices associated with the Value of Lost Load (VoLL) and Customer Damage Function (CDF). ENS, CI and CML are expressed through their expected values as well as probability and/or cumulative density functions.

For a system of components connected in series, the outage rate is given by:

$$\lambda_e = \sum_{i=1}^N \lambda_i \quad (5.1)$$

while the average outage duration is:

$$r_e = \frac{\sum_{i=1}^N \lambda_i r_i}{\lambda_e} \quad (5.2)$$

The unavailability is given by:

$$U_e = \lambda_e r_e \quad (5.3)$$

where λ_i is the fault rate of component i , r_i is the average outage duration of component i , and N is the number of components connected in series. The underlying assumption here is that repair times are much shorter than mean times between faults.

For parallel circuits, the outage rate and average outage duration are given by:

$$\lambda_e = \sum_{i=1}^N \lambda_i \prod_{j=1, j \neq i}^N \lambda_j r_j \quad (5.4)$$

$$\frac{1}{r_e} = \sum_{i=1}^N \frac{1}{r_i} \quad (5.5)$$

The contribution to the expected annual supply-outage time is

$$U_s = \lambda_e t \quad (5.6)$$

$$U_r = \lambda_e r_u \quad (5.7)$$

where t is the time to transfer part of the load by switching and r_u is the time needed to restore all supplies. Typically, r_u is less than the average outage duration r_e for a dual-circuit system.

The supply outage rate due to faults on component i overlapping with maintenance of component j is given by:

$$\lambda_m = \lambda_i \lambda_{mj} r_{mj} \quad (5.8)$$

And the contribution to annual supply-outage time is given by:

$$U_m = \lambda_m r_m \quad (5.9)$$

where λ_{mj} is the maintenance outage rate of component j , r_{mj} is the duration needed for maintenance of component j and r_m is the average time to close down maintenance work and restore the circuit being maintained.

Continuous-time Markov Chains

Continuous-time Markov Chains (CTMC) can be used to estimate stationary probabilities of each discrete system state where simpler series/parallel approach cannot be used such as, for example, in systems with multi-state components and/or common mode failures.

The CTMC is defined with a transition rate matrix between system states. Figure 13.12 shows an example of a Markov chain showing states of one main (e.g. LV feeder) and one reserve component (e.g. spare cable). In state 1 both components are in service and the load is supplied by the main component. In state 2 the main component goes out of service, while state 3 occurs after switching the supply onto the reserve component.

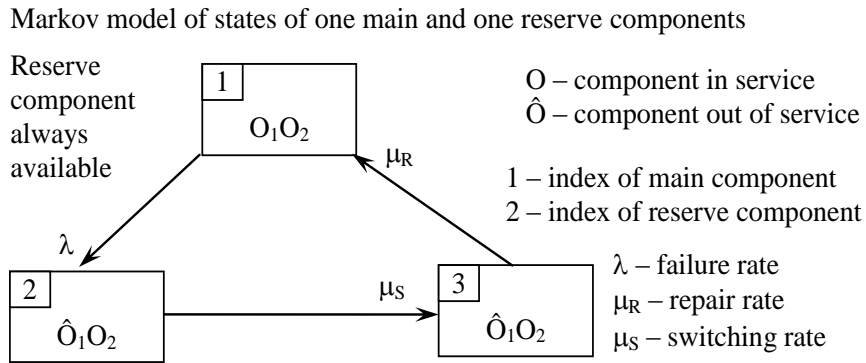


Figure 13.12: Markov model of LV feeder with a spare cable

The system goes from state 1 to state 2 when the main component fails and has to be put out of service. The transition rate between states 1 and 2 is represented by the failure rate of the main component (λ). While system is in state 2, the load is not supplied. By isolating the main component and re-establishing supply through the reserve component, the system transitions from state 2 to state 3, with the transition rate equal to the switching rate (μ_S). After the repair of the main component and switching the supply back to the main component, the system moves from state 3 to state 1, with the transition rate equal to the repair rate of the main component (μ_R). The transition rate matrix is shown below:

$$Q = \begin{bmatrix} & \lambda & \\ \mu_R & & \mu_S \end{bmatrix}. \quad (5.10)$$

The long-term stationary probability of the system residing in each system state is calculated from equations:

$$QP = 0 \quad (5.11)$$

and

$$\sum_{i=1}^N p_i = 1. \quad (5.12)$$

where N is the number of system states, p_i is the probability of system being in state i , and P is the vector of system state probabilities.

State probabilities are determined by solving the system of linear equations (5.11) and (5.12).²⁰ The resulting state probabilities are:

$$P = \frac{1}{\lambda\mu_S + \lambda\mu_R + \mu_S\mu_R} \begin{bmatrix} \mu_S\mu_R \\ \lambda\mu_R \\ \lambda\mu_S \end{bmatrix}. \quad (5.13)$$

Load interruption occurs only in state 2. The expected CML (ECML) and EENS are therefore calculated from the probability of the system being in state 2, while the Expected CI (ECI²¹) are determined from the frequency of system transitioning from state 1 to state 2:

$$ECML = 60 \cdot 8760 \frac{\lambda\mu_R}{\lambda\mu_S + \lambda\mu_R + \mu_S\mu_R} \quad (5.14)$$

²⁰ It should be noted that one of equations from (5.5.11) is omitted due to singularity.

²¹ In line with the ER P2/6 definitions, Customer Interruptions (CI) are expressed as the number of interruptions per 100 customers.

$$EENS = \frac{\lambda\mu_R}{\lambda\mu_S + \lambda\mu_R + \mu_S\mu_R} E \quad (5.15)$$

$$ECI = 100 \frac{\lambda\mu_S\mu_R}{\lambda\mu_S + \lambda\mu_R + \mu_S\mu_R} \quad (5.16)$$

Where E is the total annual demand.

On-network faults – failure effect analysis

Figure 13.13 shows the illustration of the failure effect analysis. For a fault occurring on a section marked with a broken arrow, a fault breaking device (FBD) will open and after a short time again close the circuit breaker. Immediately after the FBD opens, the automated switchgear will also open to isolate the fault. In addition, automated normally open points (NOPs) might close to restore the supply to some customers (the lavender area in Figure 13.13). Those customers will experience short supply interruptions (typically less than 60 seconds) which according to current security standard do not count towards the total CI figure. The maintenance and repair team can manually open switchgears and close NOPs, if these are not automated, and resupply customers in the orange area, effectively reducing the isolated area to the one shown in red. Supply to some or all of customers in the red area may be restored by load transfer onto a lower voltage level and/or by connecting mobile generators. The supply to remaining customers will be restored after the fault is cleared.

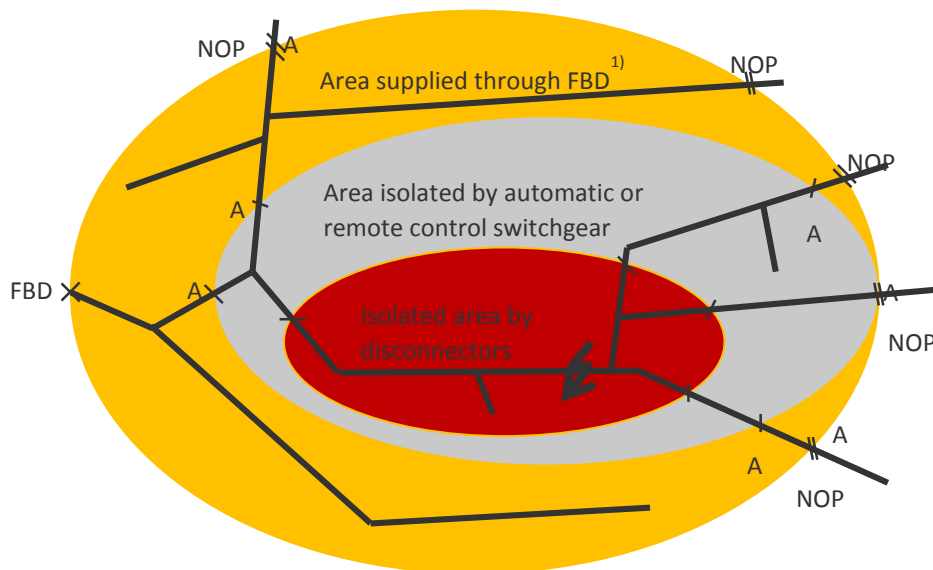


Figure 13.13: Illustration of failure effect analysis; Note 1) excludes unsupplied areas due to existing faults

The expected annual outage time, U_s , due to the outage of a single component s (or common-mode faults or faults on busbars) is given by:

$$U_s = p_0 \lambda_s t_{sl} \quad (5.17)$$

where

p_0 – probability of intact system. For systems where repair times are much shorter than the mean times between faults p_0 is close to 1 and can be omitted.

λ_s – failure rate of component s

t_{sl} – average outage duration (years) for load l due to outage of component s . It can be the expected time to resupply or transfer load by switching or mean time to repair for component s , r_s .

The expected annual outage time, U_o , due to an overlapping fault on component j while component i is being repaired is given by:

$$U_o = p_i \lambda_j t_{ul} \quad (5.18)$$

where

p_i – probability of component i being on outage

λ_j – failure rate of component j

t_{ul} – average urgent outage duration (years) for load l due to an overlapping fault on component j while component i is in the repair. This can be either the expected time to resupply or transfer load by switching or mean urgent repair time, r_u as follows:

$$r_u = f_u \frac{r_i r_j}{r_i + r_j} \quad (5.19)$$

f_u – urgent repair time factor to correct the average supply outage duration due to overlapping faults, $0 < f_u \leq 1$. In the illustrative examples it is assumed to be equal to 1.

It is assumed that the load, not supplied until component i is repaired, is not affected by the overlapping faults while loads resupplied by switching can be.

The expected annual outage time, U_3 , due to overlapping fault on component k while fault on component j overlaps repair of component i is given by:

$$U_3 = p_{ij} \lambda_k t_{u3l} \quad (5.20)$$

where:

p_{ij} – probability of overlapping fault occurring on component j while component i is in repair

t_{u3l} – average urgent outage duration (years) for load l due to an N-3 fault. This can be either the expected time to resupply or transfer load by switching or mean urgent repair time, r_{u3} as follows:

$$r_{u3} = f_u \frac{r_i r_j r_k}{r_i r_j + r_i r_k + r_j r_k} \quad (5.21)$$

The probabilities in the above expressions are calculated as follows:

$$p_0 \approx 1 - p_{n-1} \quad (5.22)$$

$$p_i \approx \lambda_i r_i \quad (5.23)$$

$$p_{ij} \approx \lambda_i r_i \lambda_j r_j \quad (5.24)$$

$$p_{ijk} \approx \lambda_i r_i \lambda_j r_j \lambda_k r_k \quad (5.25)$$

$$p_{n-1} = \sum_{i=1}^n \lambda_i r_i = \sum_{i=1}^n p_i \quad (5.26)$$

Power flow calculations are performed to estimate power flows and node voltages in the network in different conditions. For low-voltage networks the power flow also takes into account load diversity. The calculation is used to estimate whether a switching action will result in a violation of thermal and/or voltage constraints. If this is the case, the appropriate switches are identified and some load points are not re-supplied during the time violations might occur. The assumption is that a potential overload is detected by the operator investigating the consequences of load transfer by switching. Alternatively, load transfer at the lower voltage level or demand side response might enable the re-supply of load points during the time violations occur.

Disconnected load and energy lost

Assuming that fault outages occur randomly throughout the year, the average disconnected load (P_a) is obtained by multiplying the difference between maximum demand (P_m) and transferred demand (P_t) by the load factor (LF) for the relevant period, as follows:

$$P_a = (P_m - P_t)LF \quad (5.27)$$

For common-mode faults and independent faults whose outages overlap, the relevant period is the whole year, while where a fault overlaps a maintenance outage, the relevant period is the maintenance window.

The expected energy lost per year is the energy not supplied, ENS, multiplied by the relevant expected unavailability and given by:

$$E_a = ENS \cdot U. \quad (5.28)$$

When a fault occurs which leads to a potential asset overloading, the ENS (assuming excessive load is disconnected or transferred) is calculated as shown in Figure 13.14, where demand exceeds the available network capacity R (e.g. feeder rating). If the available capacity is superimposed onto the Load Duration Curve (LDC), the energy above the available capacity line (represented by the orange area) should be curtailed. This is denoted as ENS. Multiplying the ENS with the appropriate probability of the condition where load shedding is necessary (e.g. single outage where there is not enough redundancy or double outage etc.) then allows for calculating the Expected Energy Not Supplied.

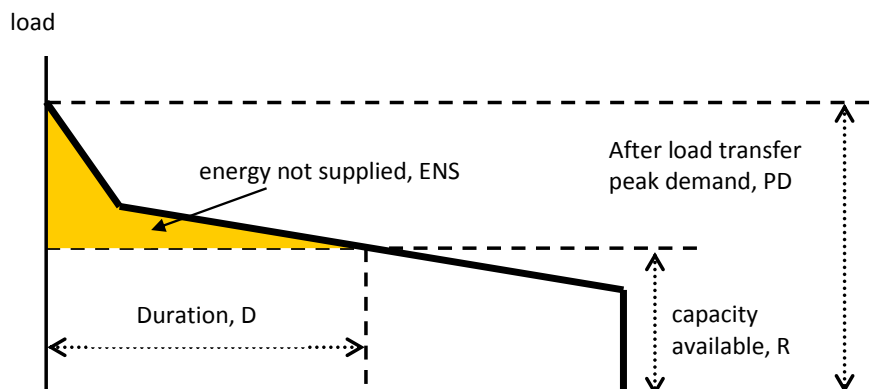


Figure 13.14: Evaluating Energy Not Supplied

The expected cost of energy not supplied overall and per load point / consumer is given by

$$C_{EENS} = CF \cdot VoLL \cdot E_a, \text{ and} \quad (5.29)$$

$$C_{EENS} = \frac{C_{EENS}}{N}. \quad (5.30)$$

Where CF is capitalisation factor for discount rate of 3.5% over 30 years followed by 15 years of 3% discount rate, $VoLL$ is the value of lost load and N is the number of consumers per load point. Over 45 years the capitalisation factor CF is around 23, which is found as the average value between cases where costs are incurred at the beginning and at the end of each year during the 45-year period.

Optimal economic design of distribution networks

Cost-benefit analysis (CBA) is the approach most commonly used to determine the economically and technically optimal design of the distribution network. Figure 13.15 shows the concept of the CBA approach that underpins ER P2/6. This approach balances the cost of outages (caused by the stochastic behaviour of the system such as e.g. component outages or failures) against investment and maintenance costs. Generally, the cost of outages reduces with increasing redundancy, as this normally mitigates the adverse effects of outages and reduces the duration and frequency of interruptions. However, the investment costs would obviously increase with the provision of increased redundancy to improve the reliability performance of the network. The optimal trade-off between the cost of interruptions and cost of investing in network capacity i.e. redundancy is reached when the incremental cost of investment and maintenance is equal to the incremental benefit from reduced cost of outages.

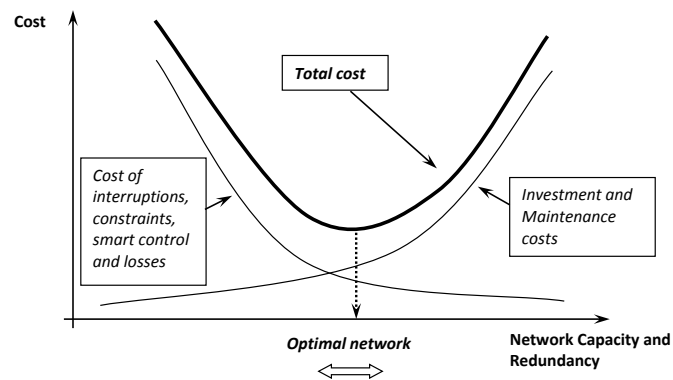


Figure 13.15: Probabilistic cost-benefits analysis framework for distribution network operation and planning (balancing of network operation costs that includes cost of service interruptions, smart control and losses against cost of investment in network assets)

Due to the stochastic nature of the reliability analysis used to determine the effects of supply interruptions, the CBA of distribution network design is fundamentally probabilistic. ER P2/6 provides a platform for conducting such an analysis for any network reinforcement and development scenario.

The effectiveness of investments with a long useful life can be estimated using the index of cost per kWh saved given by the expression below:

$$V = \frac{C_a + C_m - B_l}{E} \quad (5.31)$$

Where C_a is the capital component of not deferring expenditure for one year, C_m is the cost of operation and maintenance, B_l is the benefit of reducing losses, and E is the expected reduction of energy not served (in kWh), or energy saved, in the first year. The capital component of not deferring expenditure for one year is given by:

$$C_a = \frac{i}{1+i} \cdot C \quad (5.32)$$

Where C is the total capital cost and i is the discount rate.

13.6 Stochastic planning model for DSR

In this section we introduce the stochastic planning model, capable of minimizing expected investment cost across a scenario tree while allowing investment in transformers and DSR schemes. We first introduce the mathematical symbols used, followed by the mathematical formulation of the optimisation problem.

Nomenclature – Sets and indices

Ω_M	Set of scenario tree nodes, indexed m .
Ω_E	Set of epochs, indexed e .
Ω_{TX}	Set of existing transformers, indexed t .
ε_m	Epoch to which scenario tree node m belongs to.
Φ_m^Y	Time-ordered set containing all parents of node m , from the first stage up to stage $\varepsilon_m - \gamma$, where γ is integer

Nomenclature – Input parameters

π_m	Probability of scenario tree node m .
κ^{TX}	Annual capital cost of transformer (£/year)
κ^{DSR}	Annual capital cost of DSR scheme (£/year)
γ^{TX}	Commissioning time of a transformer.
γ^{DSR}	Commissioning time of DSR scheme.
D_m^{\max}	Peak demand at scenario tree node m (MVA).
Y^{TX}	Size of transformer (MVA).
Y^{DSR}	Contract size of DSR scheme (MVA).
α	Availability of DSR scheme $\in [0,1]$.
ζ	Security standard $\in [0,1]$.
r_e	Cumulative discount factor for investment cost at epoch e .
r	Discount rate.
y_e^*	Index of first year of epoch e ; by convention the very first year of the study horizon is 0 i.e. $y_1^* = 0$.
y_e^{**}	Index of last year of epoch e .

Nomenclature – Decision variables

B_m^{TX}	Binary variable signifying investment in a new transformer at scenario tree node m .
B_m^{DSR}	Binary variable signifying investment in DSR scheme at scenario tree node m .
\tilde{B}_m^{TX}	Aggregate binary state variable denoting presence of new transformer at node m .
\tilde{B}_m^{DSR}	Aggregate binary state variable denoting presence of DSR scheme at node m .
P_m	Amount of power that can be imported from the grid at node m (MVA).

Mathematical Formulation

$$\min_{B^{TX}, B^{DSR}} \left\{ \sum_{m \in \Omega_M} \pi_m r_{\varepsilon_m} (B_m^{TX} + B_m^{DSR}) \right\} \quad (6.1)$$

Subject to

$$(|\Omega_{TX}| + \tilde{B}_m^{TX} - \zeta) Y^{TX} \geq P_m, \quad \forall m \quad (6.2)$$

$$P_m \geq D_m^{\max} - \alpha \tilde{B}_m^{DSR}, \quad \forall m \quad (6.3)$$

$$\tilde{B}_m^{TX} = \sum_{\phi \in \Phi_m^{TX}} B_m^{TX}, \quad \forall m \quad (6.4)$$

$$\tilde{B}_m^{DSR} = \sum_{\phi \in \Phi_m^{DSR}} B_m^{DSR}, \quad \forall m \quad (6.5)$$

$$r_e = \sum_{i=y_e^*}^{y_e^{**}} \frac{1}{(1+r)^{i-1}}, \quad \forall e \quad (6.6)$$

The objective function (6.1) involves the minimization of expected discounted investment cost, expressed as the sum of investment in DSR and transformers across all scenario tree nodes, multiplied by the corresponding probability of occurrence. For each node, the appropriate discounting factor is also applied in order to model the time value of money and the fact that each stage spans several years. Constraint (6.2) states that the amount of energy that can be imported from the upstream network is defined by the security standard applied, the size and number of existing transformers as well as the number of newly-built transformers. Constraint (6.3) states that the amount of power that can be imported must be greater or equal to the maximum demand to be served, as dictated by the current scenario tree node, minus the amount that demand can be reduced through the DSR scheme, if commissioned. Equation (6.4) states that the number of newly-built transformers available at node m is equal to the aggregated number of new transformers built over all previous epochs of the corresponding scenario pat, while considering commissioning delays due to build time. A similar relation is imposed on DSR schemes via constraint (6.5). Finally, equation (6.6) determines the cumulative discount factor for each stage of the scenario tree. This computation is carried out on the basis that assets' lifetime is greater study period, but larger horizon can be accommodation with straightforward modifications.

13.7 Option Value of Soft Open Point

In this section we introduce the stochastic planning model, capable of minimizing expected investment and operational cost across a scenario tree while allowing investment in conventional asset and Soft Open Points (SOP). We first introduce the mathematical symbols used, followed by the mathematical formulation of the optimisation problem.

Nomenclature – Sets and indices

Ω_C	Set of normally-open points, indexed c
Ω_E	Set of epochs, indexed e
Ω_{DG}	Set of distributed generation units, indexed g
Ω_L	Set of distribution lines, indexed l
Ω_M	Set of scenario-tree nodes, indexed m
Ω_N	Set of system buses, indexed n

Ω_{PS}	Set of primary substations
Ω_q	Set of typical days, indexed q
Ω_T	Set of demand periods, indexed t
ε_m	Epoch to which scenario-tree node m belongs
$\Phi_k(m)$	Time-ordered set containing all parent nodes of scenario-tree node m , from the first epoch up to epoch $\varepsilon_m - k$

Nomenclature – Input parameters

γ_B	Annuitized investment cost for reconductoring a distribution line l (£/year)
γ_S	Annuitized SOP investment cost (£/year)
δ_t	SOP efficiency factor
η_f	Duration of one period (hours).
π_m	Probability of scenario-tree node m occurring.
$\Psi_{n,t}$	Tangent of the load angle at bus n at period t
$\zeta_{t,g}$	Percentage output of intermittent generator g at period t relative to its installed capacity
b_l^0	Line susceptance before reinforcement (pu)
b_l^N	Line susceptance after reinforcement (pu)
c^c	Cost of curtailing DG output (£/pu · h)
F_{max}	Extra capacity, obtained from reconductoring, relative to the existing capacity (pu)
F_l	Existing capacity of line l (pu)
g_l^0	Line conductance before reinforcement (pu)
g_l^N	Line conductance after reinforcement (pu)
$I_{n,g}$	Signifies if generator g is connected to bus n
$d_{t,n}$	Real power demand at bus n , period t (pu)
k_L	Build time for distribution line l (epochs)
k_S	Build time for SOP (epochs)
N_q	Frequency of typical day q in a year (days)
n_c^x	The two terminals ($x = a, b$) of SOP which is installed at normally-open point c
$p_{m,g}^{max}$	Max real power stable generation of g (pu)
$Q_{m,g}^{max}$	Max reactive power stable generation of g (pu)
$r_{\varepsilon_m}^I$	Cumulative discount factor for investment cost
$r_{\varepsilon_m}^O$	Cumulative discount factor for operational cost
p_c^{max}	Real power capacity of SOP installed at c (pu)
Q_c^{max}	Reactive capacity of SOP installed at c (pu)
u_l	Sending bus of line l
v_l	Receiving bus of line l
V_{set}	Voltage setpoint value at primary substation (pu)
V_{min}	Minimum voltage statutory limit (pu)
V_{max}	Maximum voltage statutory limit (pu)

Nomenclature – Decision variables

$\theta_{m,t,n}$	Voltage angle corresponding to bus n (rad)
$B_{m,l}$	Binary variable for deciding to reductor l

$\tilde{B}_{m,l}$	State variable of reconductoring line l
$\tilde{F}_{m,l}$	State variable representing the extra capacity due to reconductoring of line l (pu)
$H_{m,t,c}$	Real power drawn by SOP at terminal n_c^a (pu)
$H_{m,t,c,n}^Q$	Reactive power drawn by SOP at terminal n (pu)
$R_{m,t,c}$	Real power drawn by SOP at terminal n_c^b (pu)
$P_{m,t,g}$	Real power output of unit g (pu)
$P_{m,t,l}^S$	Real power flow at sending bus of line l (pu)
$P_{m,t,l}^R$	Real power flow at receiving bus of line l (pu)
$Q_{m,t,g}$	Reactive power output of unit g (pu)
$Q_{m,t,l}^S$	Reactive power flow at sending bus of l (pu)
$Q_{m,t,l}^R$	Reactive power flow at receiving bus of l (pu)
$S_{m,c}$	Binary variable for deciding to invest in SOP
$\tilde{S}_{m,c}$	State variable of SOP investment
$V_{m,t,n}$	Voltage magnitude at bus n (pu)

Mathematical Formulation

$$z = \min_{B, C, D, S} \left\{ \sum_{m \in \Omega_M} \pi_m (r_{\varepsilon_m}^I \omega_m^I + r_{\varepsilon_m}^O \omega_m^O) \right\} \quad (7.1)$$

subject to

$$\omega_m^I = \sum_{l \in \Omega_L} B_{m,l} \gamma_B + \sum_{c \in \Omega_C} S_{m,c} \gamma_S, \quad \forall m \quad (7.2)$$

$$\omega_m^O = \sum_{t \in \Omega_T} \sum_{q \in \Omega_Q} N_q \delta_t c^c \sum_{g \in \Omega_{DG}} (P_{m,g}^{\max} \zeta_{t,g} - P_{m,t,g}), \quad \forall m \quad (7.3)$$

$$\tilde{B}_{m,l} = \sum_{\varphi \in \Phi_{k_L}(m)} B_{\varphi,l}, \quad \forall m, l \quad (7.4)$$

$$\tilde{F}_{m,l} = \sum_{\varphi \in \Phi_{k_L}(m)} B_{\varphi,l} F_{\max}, \quad \forall m, l \quad (7.5)$$

$$\tilde{S}_{m,c} = \sum_{\varphi \in \Phi_{k_S}(m)} S_{\varphi,c}, \quad \forall m, c \quad (7.6)$$

$$P_{m,t,g} \leq P_{m,g}^{\max}, \quad \forall m, t, g \in \Omega_{PS} \quad (7.7)$$

$$Q_{m,t,g} \leq Q_{m,g}^{\max}, \quad \forall m, t, g \in \Omega_{PS} \quad (7.8)$$

$$P_{m,t,g} \leq P_{m,g}^{\max} \cdot \zeta_{t,g}, \quad \forall m, t, g \in \Omega_{DG} \quad (7.9)$$

$$Q_{m,t,g} \leq Q_{m,g}^{\max} \cdot \zeta_{t,g}, \quad \forall m, t, g \in \Omega_{DG} \quad (7.10)$$

$$P_{m,t,l}^S = (1 - \tilde{B}_{m,l}) [V_{m,t,u_l}^2 g_l^O - V_{m,t,u_l} V_{m,t,v_l} g_l^O]$$

$$\cos(\theta_{m,t,u_l} - \theta_{m,t,v_l}) - V_{m,t,u_l} V_{m,t,v_l} b_l^O \sin(\theta_{m,t,u_l} - \theta_{m,t,v_l}) + \tilde{B}_{m,l} [V_{m,t,u_l}^2 g_l^N - V_{m,t,u_l} V_{m,t,v_l} g_l^N \cos(\theta_{m,t,u_l} - \theta_{m,t,v_l}) - V_{m,t,u_l} V_{m,t,v_l} b_l^N \cdot \sin(\theta_{m,t,u_l} - \theta_{m,t,v_l})], \quad \forall m, t, l \quad (7.11)$$

$$P_{m,t,l}^R = (1 - \tilde{B}_{m,l}) [V_{m,t,v_l}^2 g_l^O - V_{m,t,v_l} V_{m,t,u_l} g_l^O]$$

$$\cos(\theta_{m,t,v_l} - \theta_{m,t,u_l}) - V_{m,t,u_l} V_{m,t,v_l} b_l^O \sin(\theta_{m,t,v_l} - \theta_{m,t,u_l}) + \tilde{B}_{m,l} [V_{m,t,v_l}^2 g_l^N - V_{m,t,u_l} V_{m,t,v_l} g_l^N \cos(\theta_{m,t,v_l} - \theta_{m,t,u_l}) - V_{m,t,u_l} V_{m,t,v_l} b_l^N \cdot \sin(\theta_{m,t,v_l} - \theta_{m,t,u_l})], \quad \forall m, t, l \quad (7.12)$$

$$\begin{aligned}
Q_{m,t,l}^s &= (1 - \tilde{B}_{m,l})[-V_{m,t,u_l}^2 b_l^o - V_{m,t,u_l} V_{m,t,v_l} g_l^o \cdot \\
&\sin(\theta_{m,t,u_l} - \theta_{m,t,v_l}) + V_{m,t,u_l} V_{m,t,v_l} b_l^o \cos(\theta_{m,t,u_l} - \theta_{m,t,v_l})] \\
&+ \tilde{B}_{m,l}[-V_{m,t,u_l}^2 b_l^N - V_{m,t,u_l} V_{m,t,v_l} g_l^N \sin(\theta_{m,t,u_l} - \theta_{m,t,v_l}) \\
&+ V_{m,t,u_l} V_{m,t,v_l} b_l^N \cos(\theta_{m,t,u_l} - \theta_{m,t,v_l})] \\
Q_{m,t,l}^r &= (1 - \tilde{B}_{m,l})[-V_{m,t,v_l}^2 b_l^o - V_{m,t,u_l} V_{m,t,v_l} g_l^o \cdot \\
&\sin(\theta_{m,t,v_l} - \theta_{m,t,u_l}) + V_{m,t,u_l} V_{m,t,v_l} b_l^o \cos(\theta_{m,t,v_l} - \theta_{m,t,u_l})] \\
&+ \tilde{B}_{m,l}[-V_{m,t,v_l}^2 b_l^N - V_{m,t,u_l} V_{m,t,v_l} g_l^N \sin(\theta_{m,t,v_l} - \theta_{m,t,u_l}) \\
&+ V_{m,t,u_l} V_{m,t,v_l} b_l^N \cos(\theta_{m,t,v_l} - \theta_{m,t,u_l})]
\end{aligned} \quad , \forall m, t, l \quad (7.13)$$

$$\begin{aligned}
&+ V_{m,t,u_l} V_{m,t,v_l} b_l^N \cos(\theta_{m,t,u_l} - \theta_{m,t,v_l})] \\
(P_{m,t,l}^{s,r})^2 + (Q_{m,t,l}^{s,r})^2 &\leq [F_l + \tilde{F}_{m,l}]^2 \quad , \forall m, t, l \quad (7.15) \\
V_{min} &\leq V_{m,t,n} \leq V_{max} \quad , \forall m, t, n - \{1\} \quad (7.16) \\
V_{m,t,1} &= V_{set} \quad , \forall m, t \quad (7.17) \\
R_{m,t,c} &\leq P_c^{max} \cdot \tilde{S}_{m,c} \quad , \forall m, t, c \quad (7.18) \\
H_{m,t,c} &\leq P_c^{max} \cdot \tilde{S}_{m,c} \quad , \forall m, t, c \quad (7.19) \\
|H_{m,t,c,n}^Q| &\leq Q_c^{max} \cdot \tilde{S}_{m,c} \quad , \forall m, t, c \quad (7.20)
\end{aligned}$$

$$\sum_{g \in \Omega_g} P_{m,t,g} I_{n,g} - \sum_{l \in \{\Omega_L | v_l = n\}} P_{m,t,l}^r - \sum_{l \in \{\Omega_L | u_l = n\}} P_{m,t,l}^s =$$

$$+ d_{t,n} + \sum_{c \in \{\Omega_C | n = n_c^a\}} (H_{m,t,c} - R_{m,t,c} \eta_f) + \sum_{c \in \{\Omega_C | n = n_c^b\}} (R_{m,t,c} - H_{m,t,c} \eta_f) \quad , \forall m, t, n \quad (7.21)$$

$$- H_{m,t,c} \eta_f)$$

$$\sum_{g \in \Omega_g} Q_{m,t,g} I_{n,g} - \sum_{l \in \{\Omega_L | v_l = n\}} Q_{m,t,l}^r - \sum_{l \in \{\Omega_L | u_l = n\}} Q_{m,t,l}^s =$$

$$+ \Psi_{n,t} d_{t,n} + \sum_{c \in \{\Omega_C | n = n_c^a \text{ or } n = n_c^b\}} H_{m,t,c,n}^Q \quad , \forall m, t, n \quad (7.22)$$

$$$$

$$$$

$$$$

$$$$

$$$$

$$$$

$$$$

$$$$

$$$$

The objective function is given by (7.1) describing the minimization of the discounted expected investment (7.2) and operational (7.3) cost. Constraints (7.4) and (7.6) define the state variables that aggregate all investment decisions taken in previous epochs while also considering the corresponding commissioning delays. Constraints (7.7) and (7.8) set the upper limits for the real and reactive power that flow through the primary substation transformer, while (7.9) and (7.10) represent the real and reactive generation of DG units. Constraints (7.11)-(7.14) express the AC power flow equations in the form of a disjunctive formulation dependent on state variable $\tilde{B}_{m,l}$ in order to capture the effect that reconductoring has on a line's electrical characteristics b_l and g_l . Note that different variables are used to model the flow at the sending and receiving ends of each; differences between these variables represent losses over the line. Constraint (7.15) states that real and reactive power flows cannot exceed the line's thermal rating. This constraint can be relaxed and expressed linearly or approximated in a piecewise-linear form. Constraint (7.16) defines the statutory voltage limits for all system buses, with the exception of the substation busbar ($n = 1$) where the OLTC

keeps the voltage at a set-point V_{set} , as in (7.17). Modelling the OLTC in this manner guarantees that the optimal value of the substation voltage will not be affected by any other bus voltage across the network, given that the OLTC does not have visibility of network parameters. Constraints (7.18) - (7.20) impose the upper bounds for the real and reactive power that a SOP can absorb or generate. The position of the SOP in the network is defined by its two terminals (or ports) n_c^a and n_c^b corresponding to the normally open point c . Then, the variables $R_{m,t,c}$ and $H_{m,t,c}$ that can only assume positive values, are used to model the ability of a SOP to transfer active power in any direction between its two terminals with efficiency η_f . The SOP can also absorb or generate reactive power at any of its two terminals. Finally, (7.21) and (7.22) ensure application of the second Kirchhoff law at every system bus.

13.8 Integrating uncertainty into security standards: Min-max regret approach

This appendix outlines the min-max regret methodology employed for determining the optimal network reinforcement decisions under uncertainty in demand growth.

For clarity purposes, a simple 2-bus general network is used in the presented formulation. The first bus corresponds to the primary of a MV/LV substation while the second bus corresponds to the point of connection of the demand. The planning problem involves the determination of the optimal capacity of the transformer and the distribution feeder connecting the two buses. For simplicity reasons, a DC power flow approximation is used. The examined investment problem is a multi-stage one, meaning that decisions about investment in transformer and feeder capacity are taken at different snapshots of the future horizon of the problem.

The min-max regret approach first solves a deterministic version of the problem for each of the different demand growth scenarios. For this reason, Section 1 below presents this deterministic formulation and Section 2 details the adopted min-max regret optimisation.

Section 1: Deterministic formulation

Objective function:

$$\min f(\mathbf{x}) = \min \sum_{s=1}^S (u_s^{ln} * (C_s^{ln,fx} + C_s^{ln,vr} * F_s^{ln}) + u_s^{tr} * (C_s^{tr,fx} + C_s^{tr,vr} * F_s^{tr})) \quad (8.1)$$

The objective function (1) represents the total investment cost of the network. The first term represents the total cost of feeder capacity, while the second one represents the total cost of transformer capacity.

Decision variables:

$$u_s^{ln}, s=1, \dots, S$$

$$u_s^{tr}, s=1, \dots, S$$

$$F_s^{ln}, s=1, \dots, S$$

$$F_s^{tr}, s=1, \dots, S$$

x denotes the vector of all decision variables of the problem

Constraints:

$$-(F^{ln,0} + \sum_{s=1}^r F_s^{ln}) \leq P_r^{dem} \leq (F^{ln,0} + \sum_{s=1}^r F_s^{ln}) \quad , \quad r=1, \dots, R \quad (8.2)$$

$$-(F^{tr,0} + \sum_{s=1}^r F_s^{tr}) \leq P_r^{dem} \leq (F^{tr,0} + \sum_{s=1}^r F_s^{tr}) \quad , \quad r=1, \dots, R \quad (8.3)$$

Constraints (2) and (3) represent the maximum flow limits on the feeder and the transformer respectively, dictated by the respective available capacity.

$$0 \leq F_s^{ln} \leq u_s^{ln} * F_s^{ln,max} \quad , \quad s=1, \dots, S \quad (8.4)$$

$$0 \leq F_s^{tr} \leq u_s^{tr} * F_s^{tr,max} \quad , \quad s=1, \dots, S \quad (8.5)$$

$$0 \leq \sum_{s=1}^S F_s^{ln} \leq F^{ln,max} \quad (8.6)$$

$$0 \leq \sum_{s=1}^S F_s^{tr} \leq F^{tr,max} \quad (8.7)$$

These constraints express potential maximum limits of the feeder and transformer capacity that can be built at each snapshot (8.4)-(8.5) and over the whole examined horizon (8.6)-(8.7).

Nomenclature:

s : Index of investment snapshots, $s=1, \dots, S$

r : Index of time windows between snapshots, $r=1, \dots, R$

u_s^{ln} : Binary variable expressing whether a feeder investment is carried out at snapshot s ($u_s^{ln}=1$) or not ($u_s^{ln}=0$)

u_s^{tr} : Binary variable expressing whether a transformer investment is carried out at snapshot s ($u_s^{tr}=1$) or not ($u_s^{tr}=0$)

$C_s^{ln,fx}$: Fixed cost of feeder investment at snapshot s (£)

$C_s^{tr,fx}$: Fixed cost of transformer investment at snapshot s (£)

$C_s^{ln,vr}$: Variable cost of feeder investment at snapshot s (£/MW)

$C_s^{tr,vr}$: Variable cost of transformer investment at snapshot s (£/MW)

F_s^{ln} : Feeder capacity built at snapshot s (MW)

$F_s^{ln,max}$: Maximum feeder capacity that can be built at snapshot s (MW)

$F^{ln,max}$: Maximum feeder capacity that can be built over the whole horizon (MW)

$F^{ln,0}$: Existing feeder capacity before the first snapshot (before the beginning of the examined horizon) (MW)

F_s^{tr} : Transformer capacity built at snapshot s (MW)

$F_s^{tr,max}$: Maximum transformer capacity that can be built at snapshot s (MW)

$F^{tr,max}$: Maximum transformer capacity that can be built over the whole horizon (MW)

$F^{tr,0}$: Existing transformer capacity before the first snapshot (before the beginning of the examined horizon) (MW)

P_r^{dem} : Active power consumption of demand at window r (MW)

Section 2: Min-max regret optimisation

As discussed above, different demand growth scenarios are considered in order to capture the relevant uncertainty. Under the adopted min-max regret approach, the deterministic problem (8.1)-(8.7) is initially solved for each of the different scenarios separately. The optimal value of the decision variable vector at each scenario i is denoted by x_i^* .

In the context of the examined problem, the min-max regret approach minimizes the regret of the decision maker after the realization of the actual demand growth. The value of the decision variable vector at the min-max regret solution is denoted by x^{MR} and is computed through the solution of the following optimization problem (where z denotes a slack variable):

Objective function:

$$\min_{z, x^{MR}} z \quad (8.8)$$

Constraints:

$$z \geq f(x^{MR}) - f(x_i^*), \quad \forall i \quad (8.9)$$

(2)-(7) for x^{MR}

13.9 Contribution to Security of Supply if DSR Cannot Run in Islanding Operation

To illustrate the operation of DSR under islanding conditions, an example system shown in Figure 13.16 is used. Group demand is supplied from two circuits of capacity T and three DSR facilities of capacity G . Assuming that critical a circuit outage is the critical condition i.e. rating of one circuit is greater than the total capacity of all units than Group Demand which can be supplied from the example system is $GD = T + 3FG$ where F is contribution factor of DSR facilities.

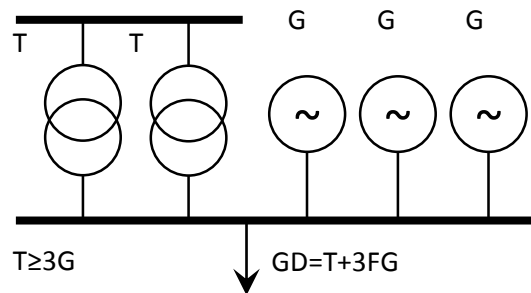


Figure 13.16: Example system shown in one bus representation; T – transformer rating, G – DSR capacity, GD – Group Demand, F – contribution factor for DSR

Capacity outage probability table for two circuits is shown in Table 13.6 while compliance probability table for three DSR facilities is shown in Table 13.7. Headers C and P are state capacity and state probability, respectively. Ptn and Pgn denote circuits and DSR facilities state probabilities, respectively, for state n.

Table 13.6: Capacity outage probability table for two circuits

C	P
2T	Pt1
T	Pt2
0	Pt3

Table 13.7: Compliance probability table for three DSR facilities

C	P
3G	Pg1
2G	Pg2
G	Pg3
0	Pg4

The capacity probability table shown in Table 13.8 is obtained by performing convolution of the circuits and DSR facilities capacity probability tables and assuming that the DSR facilities cannot run in the islanding operation. The Energy Not Supplied (ENS) is shown and E1, E2 and E3 ($E1 \leq E2 \leq E3$) are unsupplied annual energy when T+2G, T+G and T capacity is superimposed on the LDC, respectively. Depending on the contribution factor E1, E2 or E3 might be equal to zero. If contribution factor is zero then all three E1, E2 and E3 have to be equal to zero. E denotes the total annual energy demand. Given that Group Demand is a function of contribution, then E1, E2, E3, and E are functions of the contribution factor F. Multiplying ENS by the state probability and summing for all states EENS is obtained.

Table 13.8: Combined capacity probability table for two circuits and three DSR facilities if DSR facilities cannot run in islanded mode; expected energy not supplied if Group Demand is $GD = T + 3FG$

C	P	ENS	EENS
$\geq 2T$	Pt1	0	0
T+3G	Pt2 Pg1	0	0
T+2G	Pt2 Pg2	E1	E1 Pt2 Pg2
T+G	Pt2 Pg3	E2	E2 Pt2 Pg3
T	Pt2 Pg4	E3	E3 Pt2 Pg4
0	Pt3	E	E Pt3

Figure 13.17 shows the system when three DSR facilities are replaced by the equivalent firm capacity equal to $EFC = 3FG$, where F is contribution factor and G is the capacity of a single DSR facility.

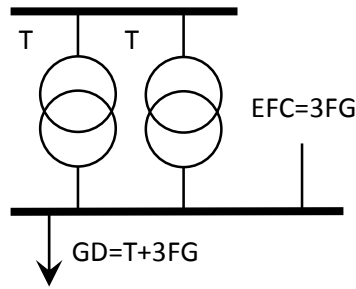


Figure 13.17: Equivalent system to one shown in Figure 13.16 where three DSR facilities are replaced by firm capacity which never fails; T – transformer rating, GD – Group Demand, G – capacity of one DSR facility, F – contribution factor, EFC – Equivalent Firm Capacity

For ELCC approach the EENS is compared with the situation if the adequate Group Demand, $GD' = T$, is supplied by two circuits only. Table 13.9 shows capacity outage probability table for this case. Given that the GD' is less than or equal to GD in Figure 13.16 the E' is less than or equal to E in Table 13.8. Hence the same conclusion is valid EENS are only the same if contribution factor is zero in which case $GD' = GD$, $E' = E$ and $E1 = E2 = E3 = 0$.

Table 13.9: Capacity outage probability table for two circuits and expected energy not supplied if Group Demand is $GD' = T$

C	P	ENS	EENS
2T	Pt1	0	0
T	Pt2	0	0
0	Pt3	E'	$E' Pt3$

It should be noted that it is assumed that demand-led DSR is implicitly delivered under islanding condition.

13.10 Dynamic Line Rating

The impact of increased convective cooling due to wind on the bare Over Head Line (OHL) conductor is modelled as a function of normalised wind power output. The modelling approach [154] is relatively conservative as it assumes that the system must be planned to cope with the maximum wind power output at minimum wind speed (rated wind speed ~14 m/s). During the operational time scale, higher wind speed beyond the rated wind speed will provide higher cooling effect which increases further the dynamic capacity of the circuit. This is considered as additional operating margin.

The increased thermal capacity is expressed as the ratio between the thermal capacity of the respective conductor with and without convective cooling due to wind. The ratio varies depending on many parameters, e.g.

- Wind speed
- Angle between wind and conductor
- Diameter of the conductor

- Ambient temperature

The calculation of this ratio is based on the IEEE standard [159] that specifies the steady state heat balance. The CIGRE model, which is in principle equivalent to the IEEE model has also been considered.

The equation is written as follows:

$$I = \sqrt{\frac{q_c + q_r - q_s}{R(T_c)}}$$

Where

I : ampacity of the conductor

T_c : conductor temperature

q_c : convective cooling

q_r : radiative cooling

q_s : solar heating

There are two types of convective cooling effects for a bare conductor:

Natural

This is a cooling effect primarily caused by lower ambient temperature. However, if the ambient temperature is higher than the temperature of the conductor, it will contribute to increase of conductor temperature. The natural cooling effect can be formulated as follows:

$$q_{cn} = 0.0205\rho_f^{0.5}D^{0.75}(T_c - T_a)^{1.25}$$

Forced

This cooling effect is primarily due to wind. It is sensitive to the wind speed, wind direction to the conductor, the ambient and the conductor temperature. The force cooling effect is calculated using following two equations:

$$q_{clow} = [1.01 + 0.0372\left(\frac{D\rho_f V_w}{\mu_f}\right)^{0.52}]k_f K_{angle}(T_c - T_a)$$

$$q_{chigh} = [0.0119\left(\frac{D\rho_f V_w}{\mu_f}\right)^{0.6}]k_f K_{angle}(T_c - T_a)$$

where:

ρ_f : air density

V_w : wind speed

μ_f : dynamic viscosity of air

k_f : thermal conductivity of air

K_{angle} : wind direction factor

D : conductor diameter

T_a : ambient temperature

T_c : temperature of the conductor

The equations provide a low and high range of the forced cooling effect; in this study, the average value between these two is used.

Curve fitting

In order to calculate the DLR capacity based on the wind power output, a curve fitting approach was employed to derive the polynomial function of the increased thermal capacity. Two 4th order polynomial functions are given in the graph below (Figure 13.18) to calculate the increased thermal capacity as a function of wind power output for a network circuit with DLR capability assuming wind direction of 0 and 90 degree.

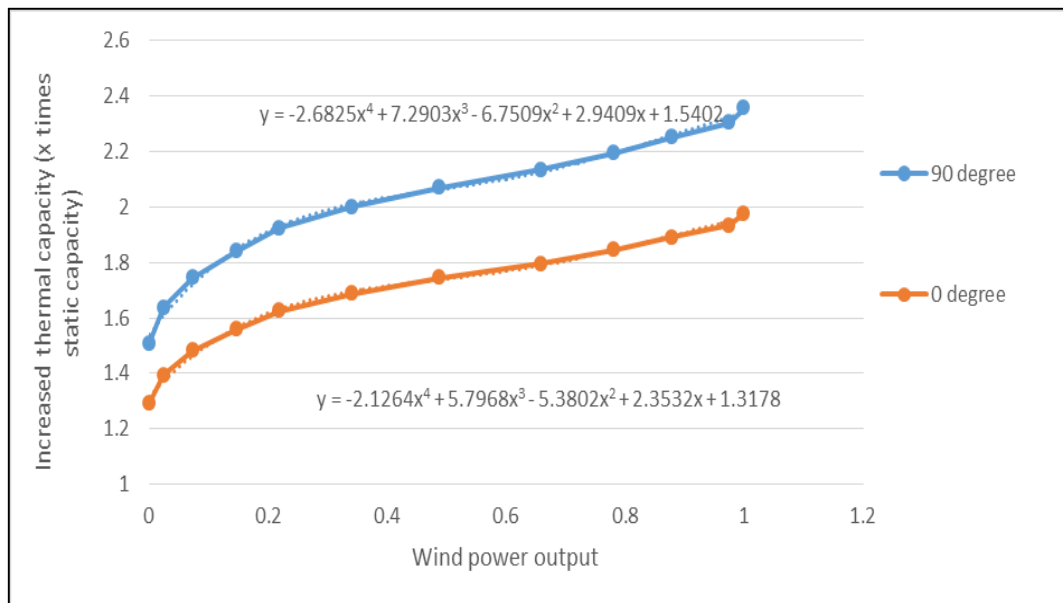


Figure 13.18: Polynomial functions to calculate the increased thermal capacity

The polynomial functions fit well with the curves. The correlation factors are above 0.996. These functions are later used in calculating the dynamic capacity of a network circuit with DLR capability. A conservative approach was adopted in the studies assuming wind direction of 0 degree. This leads to the lowest enhanced capacity as shown in Figure 13.18. Consequently, if the actual wind direction is greater than 0 degree, the temporal capacity of the circuits with DLR is higher and therefore may reduce the amount of DG curtailment, if any.

13.11 Risk assessment model – PV and reverse power flows

Cloud-cover factor distribution

The irradiance that a PV panel receives in a given moment depends on the cloud-cover conditions. A distribution of historical cloud-cover conditions is used, based on cloud-cover

factors recorded every minute during three years²². Therefore, for time intervals in which there is any potential maximum irradiance the cloud factor is defined as

$$\text{cloud factor}_t = \frac{r_t}{\bar{r}_t} \quad (11.1)$$

where r_t is the average irradiance measurement and \bar{r}_t is the clear-sky irradiance in the interval time t .

In some cases the measured irradiance may exceed the clear-sky irradiance due to a phenomenon known as the *cloud-edge effect*, in which the edges of clouds have a lens effect on the incoming solar radiation, resulting in cloud factors exceeding 1. The cloud factor is ill-defined for time intervals with near-zero clear-sky irradiance, i.e. around sunrise and sunset: small irradiance measurement errors result in large fluctuations in computed cloud factors. Those unreliable values are ignored in the construction of the cloud-cover model distribution.

Sampling of cloud-cover conditions

Our probabilistic risk assessment is based on a state sampling Monte Carlo procedure in which cloud-cover factors are sampled simultaneously for the different PV farms with a variable correlation coefficient. This method has been based on our previous work to model dependencies amongst generation levels at different wind farm [82].

The first step is to generate a correlated random sample v_1, \dots, v_5 where each value has a standard normal marginal distribution $\mathcal{N}(0,1)$. For this we use a covariance matrix defined as

$$C = \begin{pmatrix} 1 & \rho & \rho & \rho \\ \rho & 1 & \rho & \rho \\ \rho & \rho & 1 & \rho \\ \rho & \rho & \rho & 1 \end{pmatrix} \quad (11.2)$$

Each element has a variance 1 and their mutual Pearson's correlations are defined by the parameters $\rho \in [-1,1]$ (correlation between cloud conditions at the PV sites). For nearby PV farms, cloud conditions are expected to be highly correlated (correlation coefficient close to 1), but not identical (correlation strictly less than 1). For the studies, we have used the value $\rho = 0.9$.

The next step is to transform the values of the random sample to their target distributions. This is achieved by firstly converting v_1, \dots, v_5 into uniformly distributed variables between 0 and 1, using the probability integral transform $(u_1, \dots, u_5) = (F_{\mathcal{N}}(v_1), \dots, F_{\mathcal{N}}(v_5))$, where $F_{\mathcal{N}}$ is the CDF of the standard normal distribution. This is followed by an inverse probability integral transform using the historical cumulative probability distribution of the cloud-factors here referred to as F . This way, we obtain a sample set $\mathcal{S} \equiv (\mathcal{f}_1, \dots, \mathcal{f}_4) = (F^{-1}(u_1), \dots, F^{-1}(u_4))$ for the cloud cover at each PV site. In the case study, this probabilistic cloud cover model, combined with the demand curves and clear-sky irradiance pattern, results in reverse power flows that exceed the capacity of a single transformer (17MW) approx. 7.7% of the time.

²² Imperial College London, "Experiment on Photovoltaic Energy Conversion", Internal document, Dept. Elect. Eng., Imperial College London, London, UK

Risk assessment model

The samples produced with the method above produce a set of instantaneous cloud cover conditions for the PV sites. Transformer faults are characterised by the fault rates, with an explicit provision for a common mode failure (at the distribution bus) that results in a simultaneous outage of both transformers. Under these considerations, the annual fault cost exposure is computed as the sum of the expected fault costs across all operating hours:

$$\text{expected curtailment costs} = \sum_{h=1}^{8760} \left(\frac{2\lambda_s}{8760} X_s(h) + \frac{\lambda_c}{8760} X_c(h) \right) \quad (11.3)$$

where λ_s is the annual rate of individual transformer faults (occurrences/year) and $X_s(h)$ denotes the expected impact in a particular hour h . Similarly, λ_c and $X_c(h)$ are respectively the annual rate and hourly impact of common mode faults.

The expected fault costs associated with a single outage for a particular hour are computed with the Monte Carlo average cost over the full set of sampled cloud conditions \mathcal{S} . Therefore,

$$X_s(h) = \frac{1}{N} \sum_{i=1}^N C_s(h, i) \quad (11.4)$$

where N is the number of samples within the sample set \mathcal{S} and $C_s(h, i)$ is the single outage fault cost associated with hour h for the sampled cloud condition i . The value of this function depends on whether the remaining transformer is overloaded (and disconnected) or not. Therefore we may write

$$C_s(h, i) = \theta(o) \cdot c_s^{\text{overload}}(h) + (1 - \theta(o)) \cdot c_s^{-\text{overload}}(h) \quad (11.5)$$

where $\theta(o)$ represents the unit step function that returns 1 when $o > 0$ and 0 otherwise, $c_s^{\text{overload}}(h)$ and $c_s^{-\text{overload}}(h)$ denote the fault cost when the remaining transformer is overloaded and when it is not, respectively. The event of overloading for a particular hour and cloud-cover sample is modelled as

$$o(h, i) = \sum_{k=1}^4 (\beta_k^i \cdot \bar{r}_h \cdot nPanels \cdot \text{eff} \cdot \text{areaPanel}) - d_h - 17MW \quad (11.6)$$

where \bar{r}_h denotes the clear-sky irradiation and d_h the load level in hour h , $nPanels$ is the number of panels per farm, $\text{eff} = 0.204$ is the efficiency of the panels and $\text{areaPanel} = 1.7 \text{ m}^2$ the area of each panel. In addition, each panel has an upper production level set to 320W.

According to our fault restoration model, when there is no post-fault overloading, the fault costs are limited to the disconnection of 2 PV farms during the repair time rE of the faulty transformer. Therefore,

$$c_s^{\text{overload}}(h) = \sum_{t=h}^{h+rE} \text{LOGR} \cdot \mu_f \cdot \bar{r}_t \cdot 2 \cdot n\text{Panels} \cdot \text{eff} \cdot \text{areaPanel} \quad (11.7)$$

where LOGR denotes the lost of revenue from generation curtailments (£/MWh). Note that the generation curtailments are approximated with the average cloud factor μ_f computed from the historical distribution described in the previous section.

On the other hand, when the remaining transformer is overloaded, the fault costs consist of the same repair-time disconnection of 2 PV farms in addition to the disconnection of all load and the other 2 PV farms over the reconnection time rC :

$$c_s^{\text{overload}}(h) = c_s^{\text{overload}}(h) + \sum_{t=h}^{h+rC} \text{LOGR} \cdot (\mu_f \cdot \bar{r}_t \cdot 2 \cdot n\text{Panels} \cdot \text{eff} \cdot \text{areaPanel}) + \text{VOLL} \cdot d_t \quad (11.8)$$

Finally, to complete equation (11.3) in case of a common mode transformer failure, the fault costs are computed according to the equation:

$$X_c(h) = \sum_{t=h}^{h+rE} \text{LOGR} \cdot (\mu_f \cdot \bar{r}_t \cdot 4 \cdot n\text{Panels} \cdot \text{eff} \cdot \text{areaPanel}) + \text{VOLL} \cdot d_t \quad (11.9)$$

13.12 Risk assessment model – Protection system for reverse power flows

When the protection system is considered, the risk assessment model iterates over all possible protection system outputs to compute curtailment costs driven by single faults. The equation for the expected fault costs associated with a single outage for a particular hour then becomes:

$$X_s(h) = \frac{1}{N} \sum_{i=1}^N \sum_{r \in R} p_r C_s(h, i, r) \quad (12.1)$$

where R signifies the set of different protection system outcomes (i.e. defined as the number of PV farms successfully tripped upon activation of the protection scheme) and p_r their respective probabilities. Note that the outcomes, and their probabilities, depend on the number of PV generators physically connected to the protection scheme.

Accordingly, in the post-fault overloading is modelled as follows:

$$o(h, i, r) = \sum_{k=1}^4 (y(k, r) \cdot \beta_k^i \cdot \bar{r}_h \cdot n\text{Panels} \cdot \text{eff} \cdot \text{areaPanel}) - d_h - 17\text{MW} \quad (12.2)$$

where $y(k, r)$ returns 1 if site k is disconnected in outcome r of the protection scheme.

13.13 The Optimal Portfolio Model

We propose to tackle the optimal portfolio problem through an optimisation model that can efficiently balance set of preventive and corrective measures to deal with high impact low probability events originated by natural catastrophes. The optimisation model fully enumerates N-1 and N-2 outages (so-called scenarios), recognising common mode failure probability caused by natural hazard. In this context, Eq. (13.1) shows probability of a double transformer outage (in a substation of 2 transformers) that may occur due to a flooding event (with a probability of $Prob_{flood}$) or any other causes that affect each transformer independently (with a probability of $1 - Prob_{flood}$).

$$Prob_{N-2} = Prob_{flood} + Prob_{T1_out} \times Prob_{T2_out} \times (1 - Prob_{flood}) \quad (13.1)$$

The model minimises in total 6 cost components in its objective function as follows:

- Up-front network investment or annuity cost of permanent network infrastructure associated with the infrastructure that functions under normal operating conditions in the intact system. Part of this infrastructure is also available post-contingency (except for that affected by the hazard);
- Energy bought from main system which accounts for the cost related to main system operation and is calculated under each contingent state and the intact system. This energy volumes are used to supply the part of demand that is not curtailed;
- Corrective network investment which corresponds to cables deployed under a given outaged state;
- Backup generation investment which corresponds to generating units deployed under a given outaged state (part of their investment cost –or rent- that can be associated with a single outage event)
- Fuel cost of backup generation associated with the fuel cost of operating backup units that function under the emergency condition; and
- Lost load associated with demand that cannot be covered through remaining network infrastructure, backup generation or cables from neighbouring substations.

Although the model is stochastic, its solutions can full comply with N-1 criterion and use network redundancy (rather than post-contingency actions such as backup generation and corrective network deployment) to prevent demand curtailment under the occurrence of credible (N-1) outages. In contrast, non-credible (rare) events are treated in a probabilistic fashion and thus covered through an optimal portfolio of measures that include post-contingency actions. The stochastic model presents one decision stage in the beginning, before uncertainty is realised, and one (two-period) post-fault stage as follows:

- Here and now, first stage: where decisions associated with up-front (permanent) network investment are taken

- Period 1, second stage: where decisions from first stage are implemented and demand is shed if not sufficient up-front network capacity was built (albeit it can be minimised by using backup generation that can be rapidly deployed). Corrective network investment is decided in this period (right after uncertainty is revealed), but implemented at the beginning of period 2.
- Period 2, second stage: where demand is shed if not sufficient up-front network capacity was built, albeit it can be minimised by using both backup generation (deployed in period 1) and corrective network investment that is implemented at the beginning of this period (but decided and built during period 1).

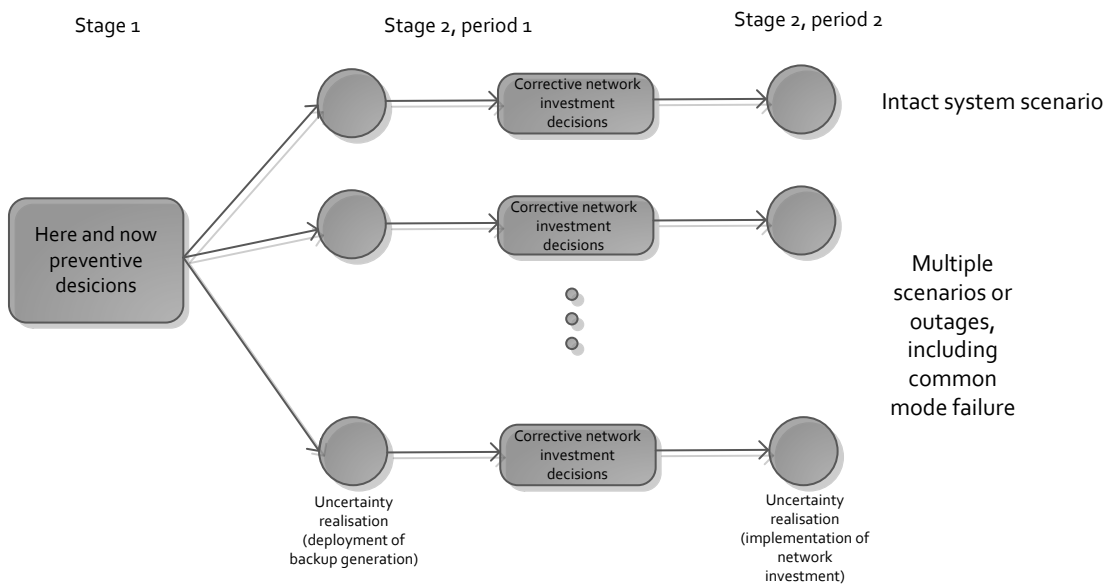


Figure 13.19: scenario tree of optimal portfolio model

13.14 Investing in Corrective Mode to Deal with High Impact Low Probability Natural Hazards

Formulation: Main equations

The model proposes new network infrastructure to be built in both preventive and corrective mode by minimising the cost of investment in preventive and corrective mode (X and Y , respectively), the cost of unsupplied demand (LL), the energy purchased from the main system (P_i) and that produced from backup generating units (P_e) in post-fault period 1 and 2 ($p=1$ and $p=2$), as shown by Eq. (14.1).

$$\text{Min} \left\{ \begin{array}{l} \sum_{l \in Nl} \pi_l^{Lp} X_l + \sum_{l \in Nl, s \in Ns} \pi_l^{Lc} Y_{l,s} \rho_s \\ \sum_{n \in Nn, s \in Ns} LL_{n,s}^{p=1} VoLL \delta^{p=1} \rho_s + \sum_{n \in Nn, s \in Ns} LL_{n,s}^{p=2} VoLL \delta^{p=2} \rho_s \\ \sum_{n \in Nn, s \in Ns} \pi_n^{Gi} \rho_s (Pi_{n,s}^{p=1} \delta^{p=1} + Pi_{n,s}^{p=2} \delta^{p=2}) \\ \sum_{n \in Nn, s \in Ns} \pi_n^{Ge.v} \rho_s (Pe_{n,s}^{p=1} \delta^{p=1} + Pe_{n,s}^{p=2} \delta^{p=2}) + \pi_n^{Ge.f} Z_{n,s} \rho_s \end{array} \right\} \quad (14.1)$$

Each post-fault period presents a supply-demand balance constraint in every node that maintains compliance with first Kirchhoff's law as shown by Eq. (2) and (3).

$$Pi_{n,s}^{p=1} + Pt_{n,s}^{p=1} = Dem_n - LL_{n,s}^{p=1} + \sum_{l \in Nl | ToNode(l)=n} F_{l,s}^{p=1} - \sum_{l \in Nl | FromNode(l)=n} F_{l,s}^{p=1}$$

$$\forall s \in Ns, n \in Nn \quad (14.2)$$

$$Pi_{n,s}^{p=2} + Pt_{n,s}^{p=2} = Dem_n - LL_{n,s}^{p=2} + \sum_{l \in Nl | ToNode(l)=n} F_{l,s}^{p=2} - \sum_{l \in Nl | FromNode(l)=n} F_{l,s}^{p=2}$$

$$\forall s \in Ns, n \in Nn \quad (14.3)$$

Power transfers must respect line rating limits according to network investments in preventive and corrective mode and this is shown in Eq. (14.4) and (14.5). Eq. (14.6) dictates that a candidate line can be built either in preventive or corrective mode.

$$|F_{l,s}^{p=1}| \leq \bar{X}_l A_{s,l} X_l \quad \forall l \in Nl, s \in Ns \quad (14.4)$$

$$|F_{l,s}^{p=2}| \leq \bar{X}_l A_{s,l} (X_l + Y_{l,s}) \quad \forall l \in Nl, s \in Ns \quad (14.5)$$

$$X_l + Y_{l,s} \leq 1 \quad \forall l \in Nl, s \in Ns \quad (14.6)$$

Disjunctive approach is used to represent compliance with second Kirchhoff's law in case a line is built and available as shown by Eq. (7)-(10). This representation also permits endogenous relaxation of the following constraints if a line is not built since M is an extremely large number. Note that when a line is built in corrective mode, it becomes available only in period 2.

$$F_{l,s}^{p=1} \leq b_l (\theta_{FromNode(l),s}^{p=1} - \theta_{ToNode(l),s}^{p=1}) + M (1 - X_l A_{s,l}) \quad \forall l \in Nl, s \in Ns \quad (14.7)$$

$$F_{l,s}^{p=1} \geq b_l (\theta_{FromNode(l),s}^{p=1} - \theta_{ToNode(l),s}^{p=1}) - M (1 - X_l A_{s,l}) \quad \forall l \in Nl, s \in Ns \quad (14.8)$$

$$F_{l,s}^{p=2} \leq b_l (\theta_{FromNode(l),s}^{p=2} - \theta_{ToNode(l),s}^{p=2}) + M (1 - (X_l + Y_{l,s}) A_{s,l}) \quad \forall l \in Nl, s \in Ns \quad (14.9)$$

$$F_{l,s}^{p=2} \geq b_l (\theta_{FromNode(l),s}^{p=2} - \theta_{ToNode(l),s}^{p=2}) - M (1 - (X_l + Y_{l,s}) A_{s,l}) \quad \forall l \in Nl, s \in Ns \quad (14.10)$$

Further equations constrain generation production to be lower than (or equal to) corresponding installed capacity and also allow us to ensure N-1 robustness (by equalising unsupplied demand variables to zero under N-1 events). All above variables are continuous and positive

except for transfers and voltage angles that can be also negative, and X, Y and Z which are binary. The model has been implemented in FICO Xpress.

Nomenclature

Parameters

$A_{s,l}$	Availability status (available or outaged) of line l during state s	0/1
b_l	Admittance of line l	[p.u.]
Dem_n	Demand in node n	[MW]
M	Large number, big M number	[MW]
$VoLL$	Value of lost load	[£/MWh]
\bar{X}_l	Rating of candidate line l	[MW]
$\delta^{p=t}$	Duration of period t	[h]
π_l^{Lp}	Investment cost of line l in preventive mode	[£/yr]
π_l^{Lc}	Investment cost of line l in corrective mode	[£/yr]
π_n^{Gi}	Energy purchase price from main system	[£/MWh]
$\pi_n^{Ge,v}$	Fuel cost of backup generating unit	[£/MWh]
$\pi_n^{Ge,f}$	Fixed cost of backup generating unit (i.e. rental fee)	[£/event]
ρ_s	Probability of state s ($s = 0$ corresponds to the intact system)	[p.u.]

Variables

X_l	Investment in line l (upfront, preventive mode)	0/1
$Y_{l,s}$	Investment in line l during state s (corrective mode)	0/1
$LL_{n,s}^{p=t}$	Lost load in node n during state s and period t	[MW]
$Pi_{n,s}^{p=t}$	Energy purchased from main system in node n during state s and period t	[MW]
$Pe_{n,s}^{p=t}$	Energy produced by backup generating unit in node n during state s and period t	[MW]
$Z_{n,s}$	Rental/use of backup generating unit in node n during state s	0/1
$F_{l,s}^{p=t}$	Power transfer through line l in state s and period t	[MW]
$\theta_{n,s}^{p=t}$	Voltage angle in node n during state s and period t	Rad

Sets

Nn	Set of nodes (equal to set of generators)
Ns	Set of states
Nl	Set of candidate lines

13.15 Consumer-driven distribution network planning

The current distribution operation and planning framework is rather centralised. The distribution network operator (DNO) makes decisions on congestion management and network upgrades without communicating with the consumers and taking into account their actual valuation of electricity supply and flexibility regarding energy use. This valuation is generally assumed identical for all consumers and identical for every unit of energy supplied, irrespectively of the specific service it provides to the consumer. Furthermore, during an outage, partial shedding of each consumer's demand is not possible; their whole demand is either served or shed, implying low reliability levels. In order to avoid network overloading

during such conditions, a portion of the consumers is completely disconnected from the network, implying unfair treatment of different consumers. Finally, the flexibility of consumers to shift in time the operation of some of their appliances is not taken into account. As a result of the above paradigm, network charges are based on long-term socialised impacts of consumers' demand on the network and do not recognise the differentiated impacts of individual consumers' choices.

The envisaged roll-out of smart metering provides a unique opportunity for consumers to communicate their individual preferences and flexibility. Building on this opportunity, a novel framework facilitating the integration of consumers' choices in distribution network operation and planning decisions has been developed. An integrated modelling approach is employed to represent two different aspects of consumers' behaviour. The first one is associated with their price elasticity i.e. the decreasing valuation of energy supply with an increasing scarcity price under outage conditions, while the second one captures their flexibility to shift the operation of their loads in time. According to the input parameters, this approach is able to model consumers' behaviour with one or both of the above aspects. This model is integrated in a distribution network planning framework with Sequential Monte Carlo (SMC) simulation of network outages to assess the impacts of consumers' behaviour.

The main conclusions stemming from case studies in different test networks examined in this report are the following:

- Higher price elasticity and shifting flexibility of consumers results in lower energy shedding costs.
- As a result, higher price elasticity and shifting flexibility tends to avoid / postpone network upgrades.
- This value of consumers' price elasticity and shifting flexibility is increased with a decreasing network reliability.
- Consumers with lower price elasticity (higher valuation of electricity supply) enjoy higher security of supply at the expense of higher network charges, while consumers with higher price elasticity (lower valuation of electricity supply) are rewarded for their lower security of supply through lower network charges.
- Consumers with higher shifting flexibility enjoy higher security of supply and network charges.

In the distribution network planning framework, the planner determines the network assets (transformers and lines) to be built or reinforced by minimising the total cost of the network within the planning horizon. This total cost is given by the summation of the annuitized investments costs associated with building / reinforcing assets and the expected annual costs of energy not supplied for the served consumers, as expressed by equation (15.1), where n is the index of years in the planning horizon, N is the length of the time horizon in years, t is the index of simulation time steps (hours) within a year, T is the size of a year in simulation time steps, and l and N_l is the index and total number of consumers in the network. This total

cost minimisation problem is subject to power flow constraints ensuring that the network operates within its thermal and voltage limits.

$$Total\ Cost = \frac{1}{N} \left(\sum_{n=1}^{n=N} \sum_{t=1}^{t=T} \sum_{l=1}^{l=N_l} DU_l(n, t) \right) + Investment\ Costs \quad (15.1)$$

Failures of network transformers and lines are modelled by employing Sequential Monte Carlo (SMC) simulation. Given the Probability Distribution Functions (PDF) of failure occurrences and duration of restoration for these network components, SMC simulation provides the state of each network component (normal operation or failure) at each time step of the planning horizon. Exponential PDF are employed in this report for modelling failure occurrences and duration of restoration, as expressed by equations (15.2) and (15.3), where λ_1 is the average number of failures per year, and λ_2 is the average duration of restoration (λ_1 and λ_2 constitute input parameters which are determined based on historical data) and τ is the index of restoration durations.

$$f_{fail}(t) = \lambda_1 e^{-\lambda_1 t} \quad (15.2)$$

$$f_{restor}(\tau) = \lambda_2 e^{-\lambda_2 \tau} \quad (15.3)$$

Two distinct modelling approaches are employed to represent the preferences and flexibility of consumers. The first one represents the valuation of different demand levels by the consumers through “price-demand” functions while the second captures their ability to shift their energy requirements in time accounting for the relevant inconvenience costs.

A piece-wise linear decreasing function is employed to model the consumers’ price demand function, which is expressed by equation (15.4), where p denotes the scarcity price, D denotes the consumers’ demand and D_b represents the consumers’ baseline demand, i.e. the demand consumers request when there is no failure in the network and the scarcity price is zero. The first section of the function -corresponding to demand levels in the interval $(0, aD_b]$ - represents the price-demand relationship for critical loads, while the second section -corresponding to demand levels in the interval $[aD_b, D_b]$ - represents the price-demand relationship for non-critical loads. The cost of energy not supplied is given by equation (5), where $\beta VoLL$ corresponds to the cost of energy not supplied for a demand level of aD_b .

$$p(D) = \begin{cases} , \forall D \leq aD_b \\ , \forall aD_b \leq D \leq D_b \\ 0, \forall D > D_b \end{cases} \quad (15.4)$$

$$DU(D) = \begin{cases} \frac{\beta VoLL}{2} D_b (1 - \alpha) + \frac{VoLL}{2\alpha D_b} ((\beta - 1)D + \alpha(1 + \beta)D_b)(\alpha D_b - D), \forall D \leq aD_b \\ \frac{\beta VoLL}{2D_b(1 - \alpha)} (D_b - D)^2, \forall aD_b \leq D \leq D_b \\ 0, \forall D > D_b \end{cases} \quad (15.5)$$

In order to capture the demand's time shifting ability, a new model has been developed by Imperial College. In this model, the demand of a consumer with shifting capability at a time period t can be reduced (implying that demand is shifted from t to another period) or increased (implying that demand is shifted from another period to t). It is assumed that demand shifting is energy neutral (i.e. the total size of demand reductions is equal to the total size of demand increases) within the time window defined by the start of an outage and 24 hours after the end of it, as expressed by equation (15.6). The cost of consumers' inconvenience for each unit of energy shifted is denoted by VoSL (value of shifting load) and defines the level of time-shifting flexibility of each consumer (a high VoSL implies low time-shifting flexibility and vice-versa), as expressed by equation (15.7).

$$\sum_{t_{start}}^{t_{end}+24} D_{shifted}(t) = 0 \quad (15.6)$$

$$Cost\ of\ Shifting = -VoSL \times \sum_{t_{start}}^{t_{end}+24} D_{shifted} \quad ,\ for\ D_{shifted} \leq 0 \quad (15.7)$$

14 APPENDIX B – DATA AND NETWORKS

The long term development statements for all GB DNOs have been used to establish the typical EHV and 132 kV networks configurations and prevailing asset characteristic used. HV network of seven DNOs have been used to estimate the typical characteristics of HV main and spur part of networks. Load profiles from Low Carbon London project and Elexon’s electricity user demand profiles have been used to establish load duration shape and typical load factors per voltage levels. Regulatory reporting pack and quality of supply reporting data are analysed. These data and in consultation with data working subgroup the range of asset upgrade cost, asset register quantity and statistic associated with network failures, outages and service restoration procedures are established.

HV feeders are split into 4 mixes as shown in Table 14.1. Mix 1 represents a system dominated with underground cables, e.g. urban systems. Mix 2 is a system with 75% or more underground cables and 25% or less overhead lines, e.g. semi-urban systems. Mix 3 and Mix 4 are systems dominated by overhead lines. The share of overhead lines in Mix 3 is less than 75% but greater than 50%, while in Mix 4, the share of overhead lines is greater than 75%. Mix 3 and Mix 4 constitute semi-rural and rural systems respectively.

Table 14.1: Systems with different mixes of underground cables and overhead lines

Percentage of	Mix 1	Mix 2	Mix 3	Mix 4
Underground cables	100%	≥75% (89% avg)	>25% (45%)	≤25% (11%)
Overhead lines	0	≤25% (11%)	<75% (55%)	≥75% (89%)

The GB HV systems are grouped into the 4 network categories (mix 1 – mix 4). For each mix, the number of HV systems is estimated and shown as a pie chart in Figure 14.1 (right). Data we have analysed show that the majority (67%) of HV feeders are Mix 1 type followed by Mix 3, Mix 4 and the last one is Mix 2 type.

Figure 14.1 (left) shows the cumulative probability of feeder’s failure rates for each of mixes. A majority of the feeders have relatively low failure rates (<0.1 occurrence per km per year). The number of networks with higher failure rates decreases, Figure 14.1 (left) shows rapid saturation for networks with failure rates more than 0.3 occurrence per km per year.

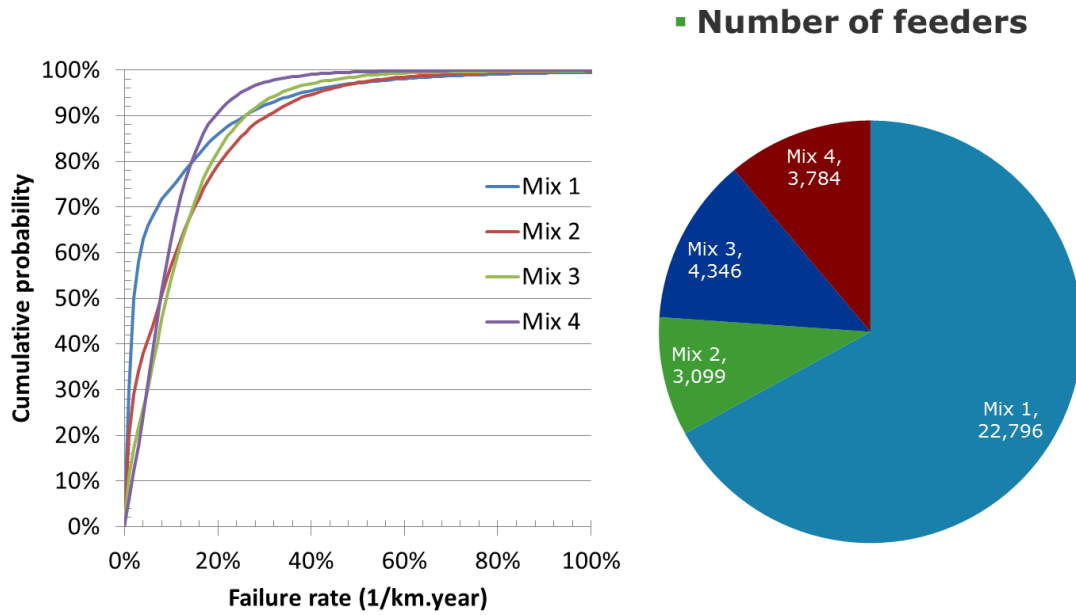


Figure 14.1: Cumulative probability of feeder's failure rates and distribution of mixes

Other details that have been modelled in the studies are the number of distribution transformers and the average distance between distribution transformers. Figure 14.2 shows the distribution for Mix 1 feeders. We find that the majority of Mix 1 feeders supply six distribution transformers with average distance of transformers between 400 and 500 m. The database contains significant number of a single supplied distribution transformer per feeder with distance to primary less than 100 m.

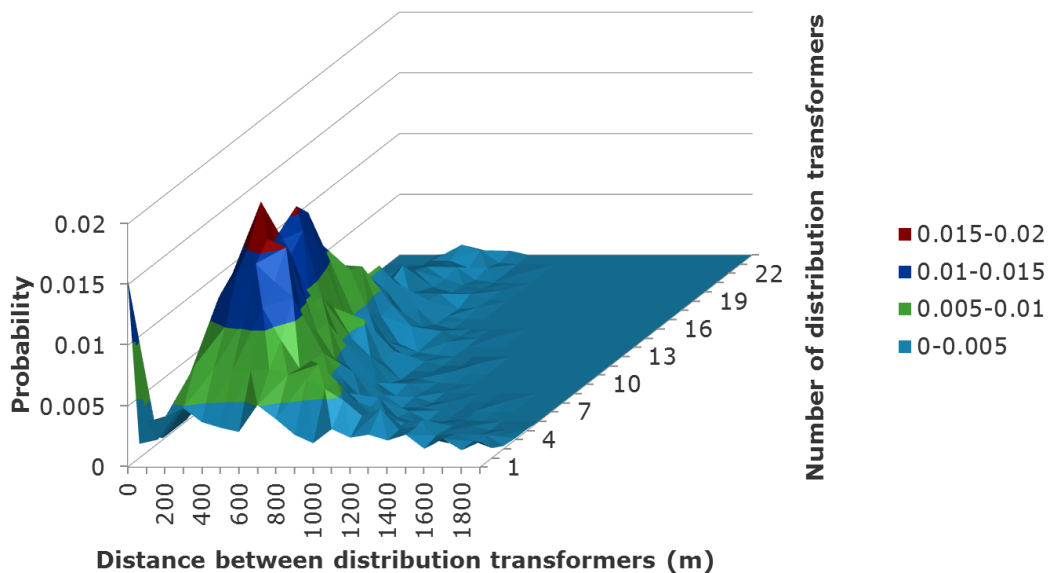


Figure 14.2: Breakdown of Mix 1 feeders per number of distribution transformers and the average distance between distribution transformers

Figure 14.3 shows the case for Mix 2 feeders. Data show that the majority of Mix 2 feeders supply 16-17 distribution transformers with the average distance between 500-600 m. This is

followed by feeders connected with 8-9 distribution transformers and 12-13 with the same average distance.

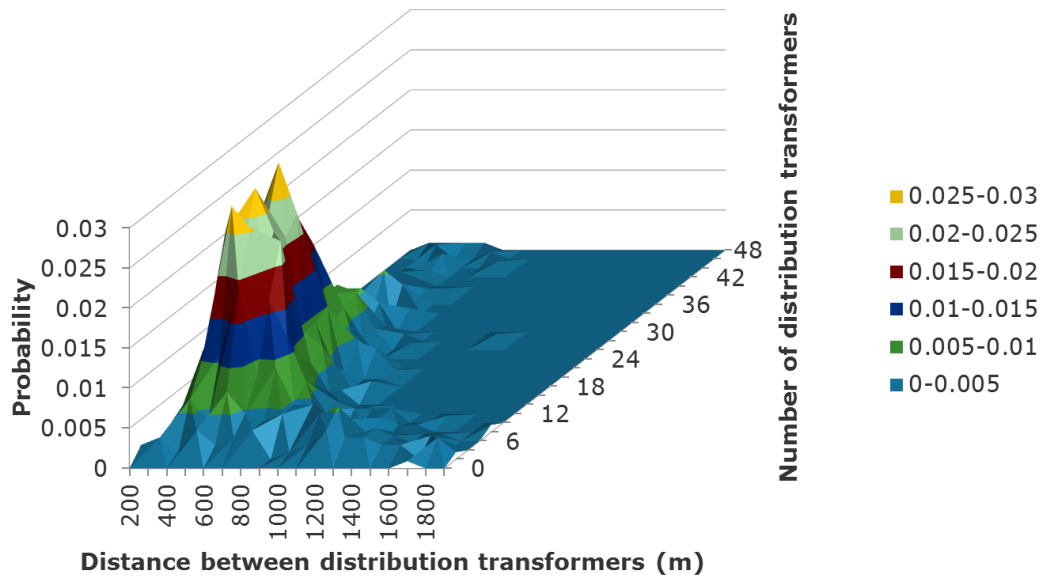


Figure 14.3: Breakdown of Mix 2 feeders per number of distribution transformers and the average distance between distribution transformers

Figure 14.4 shows the case for Mix 3 feeders. Data show that the majority of Mix 3 feeders supply 25 - 29 distribution transformers with the average distance of transformers between 500 and 600 m. This is followed by feeders connected with 15 - 19 distribution transformers with the same average distance.

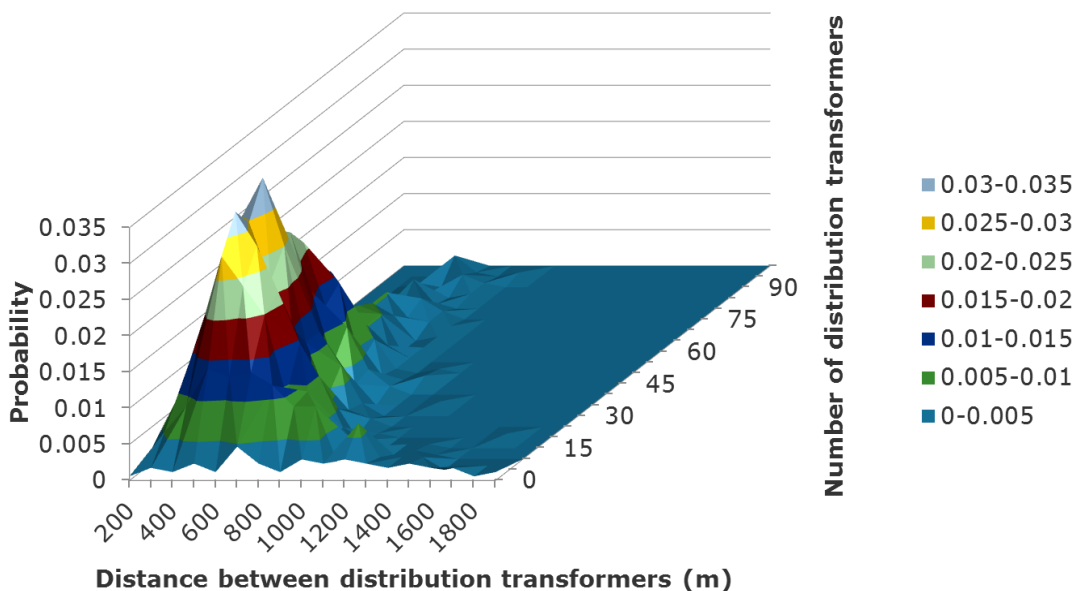


Figure 14.4: Breakdown of Mix 3 feeders per number of distribution transformers and the average distance between distribution transformers

Figure 14.5 shows the case for Mix 4 feeders. Data show that the majority of Mix 3 feeders supply 35 - 39 distribution transformers with the average distance of transformers between

600 and 700 m. This is followed by feeders connected with 15 - 19 distribution transformers with the same average distance.

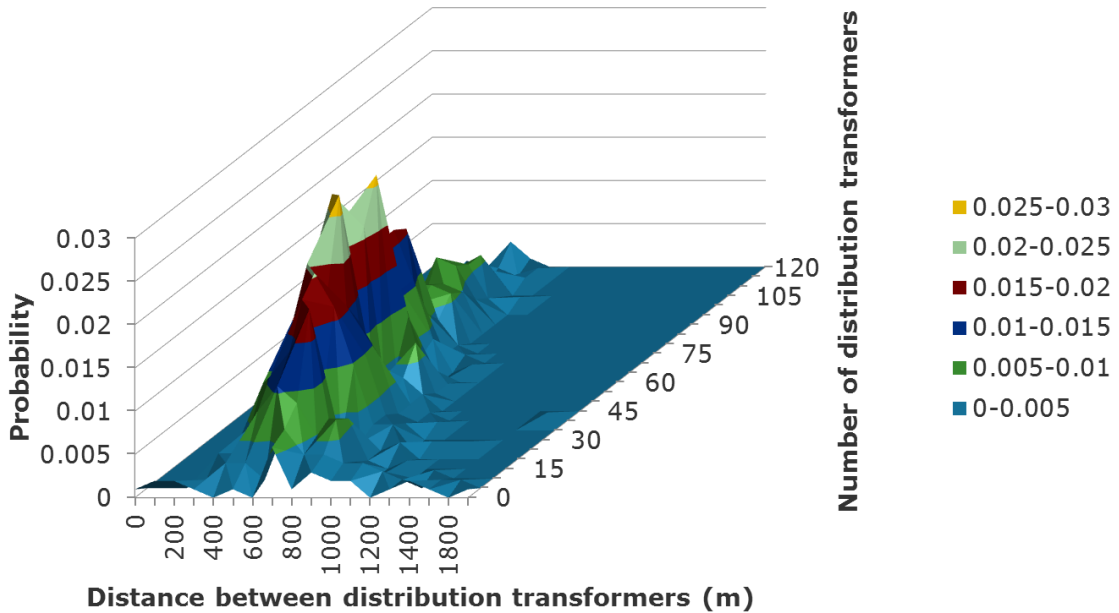


Figure 14.5: Breakdown of Mix 4 feeders per number of distribution transformers and the average distance between distribution transformers

Figure 14.6 to Figure 14.9 show distribution of average distance between distribution transformers and number of distribution transformers per HV spur for Mix 1 to 4 type of networks, respectively.

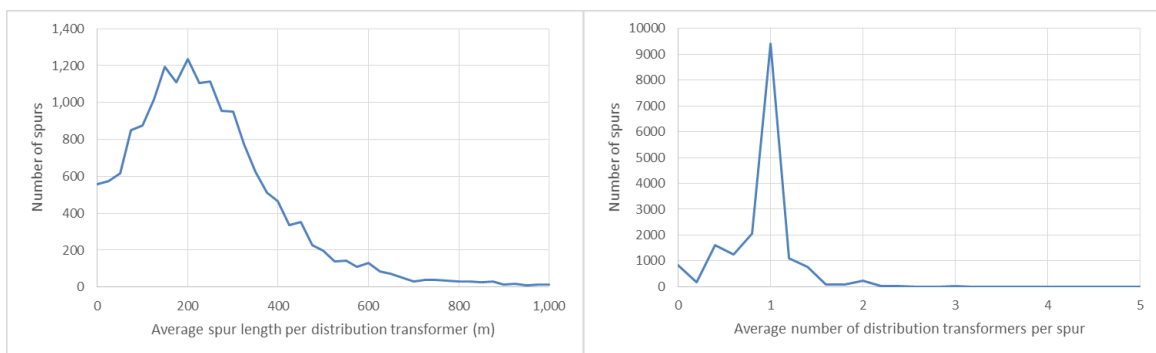


Figure 14.6: Distribution of average distance between distribution transformers and number of distribution transformers supplied from HV spur in Mix 1 type networks

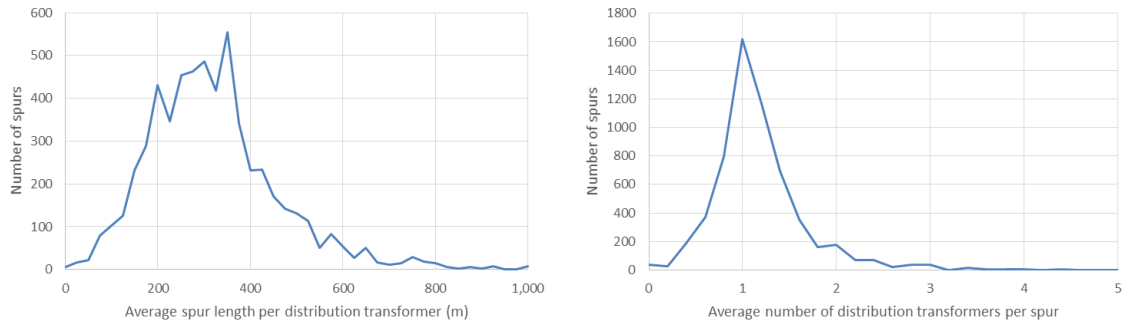


Figure 14.7: Distribution of average distance between distribution transformers and number of distribution transformers supplied from HV spur in Mix 2 type networks

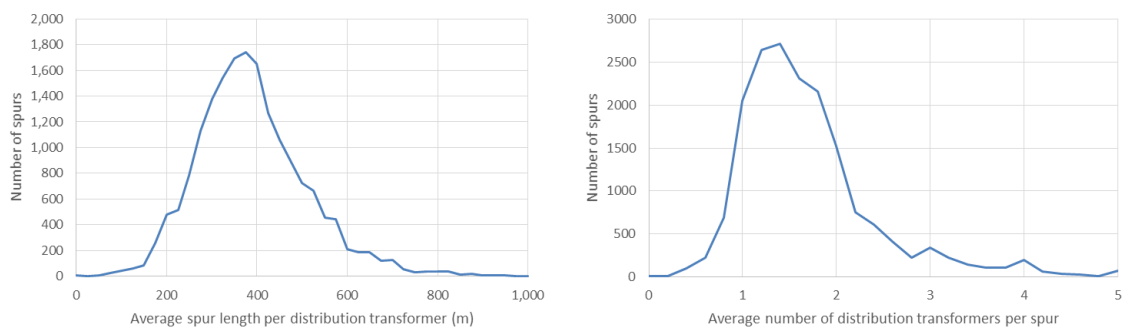


Figure 14.8: Distribution of average distance between distribution transformers and number of distribution transformers supplied from HV spur in Mix 3 type networks

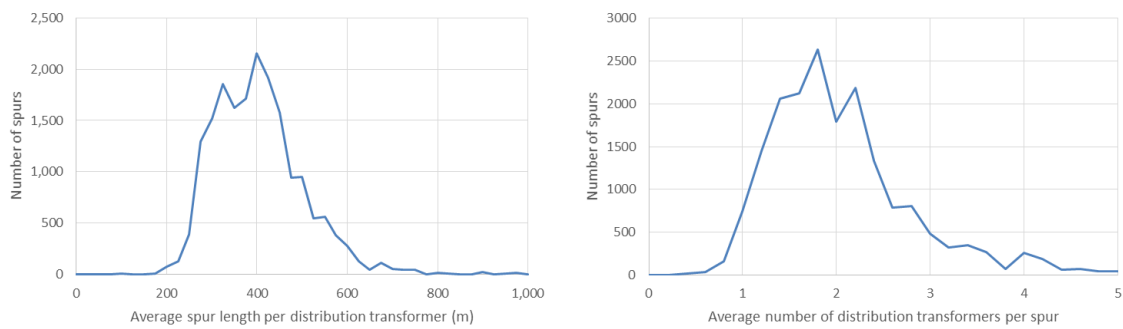


Figure 14.9: Distribution of average distance between distribution transformers and number of distribution transformers supplied from HV spur in Mix 4 type networks

Figure 14.10 shows the number of simultaneous faults per day for nine GB DNOs during five-year period.

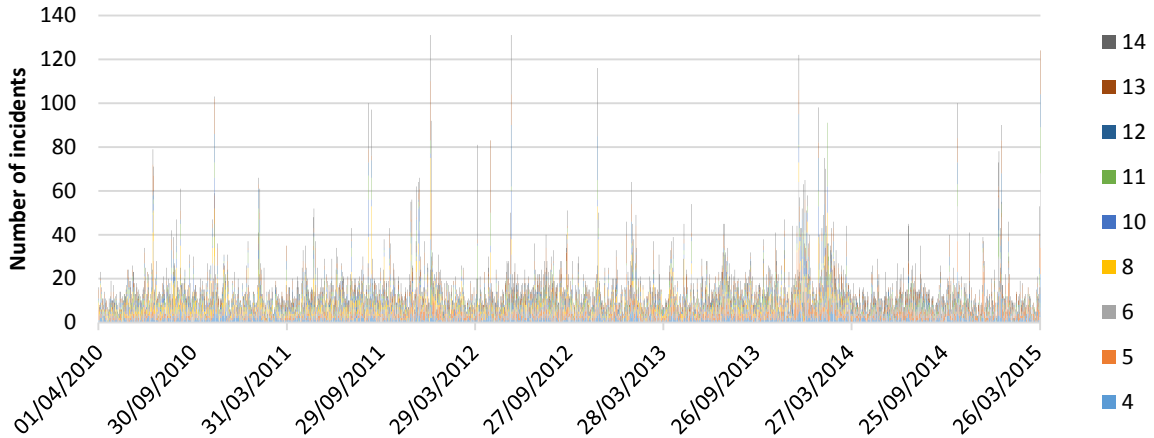


Figure 14.10: Statistics of the number of simultaneous faults per day for GB DNOs during five year period

14.1 Typical network topologies

Figure 14.11 show illustration of EHV test network supplying, as shown, three primary substations and the options connection to adjacent network.

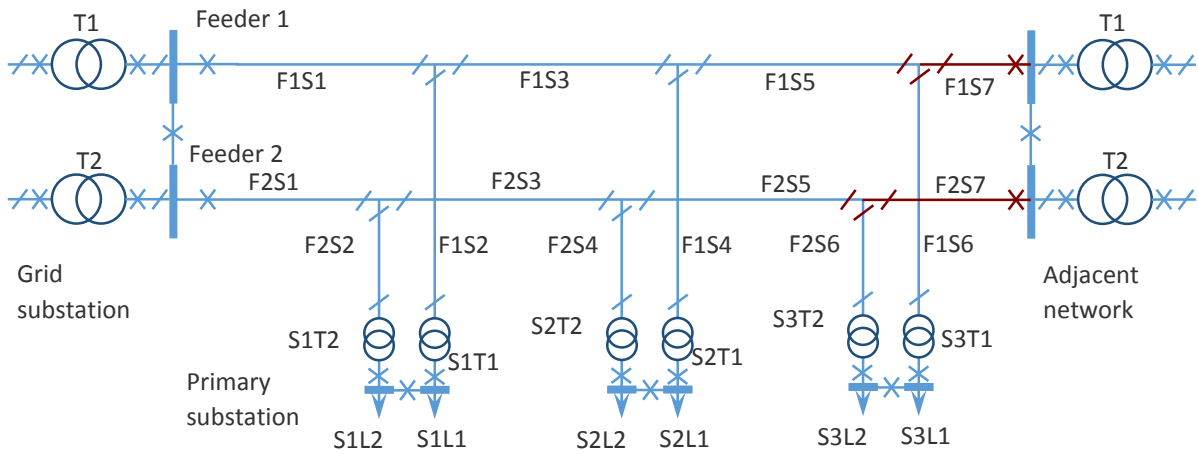


Figure 14.11: Illustration of EHV test network showing case with 3 primary substations and the optional connection to adjacent network

Figure 14.12 shows illustration of HV test network with different design redundancy options.

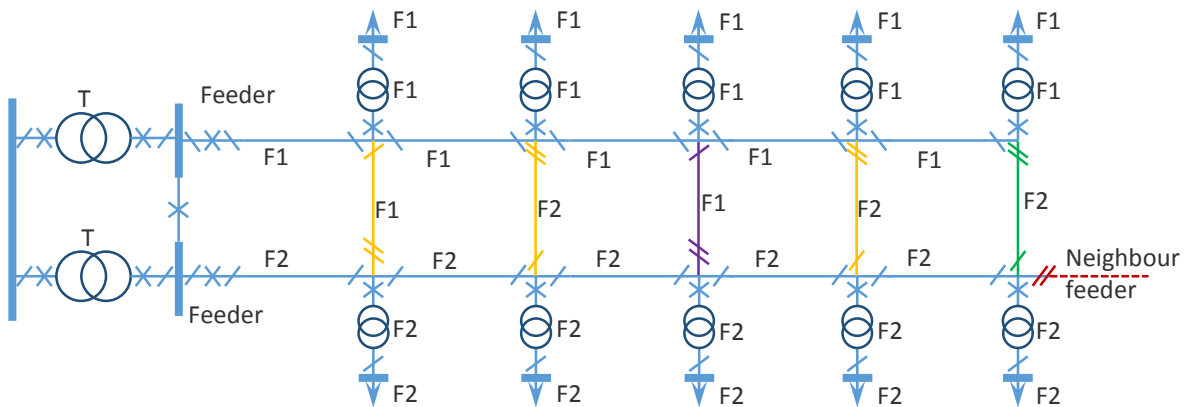


Figure 14.12: Illustration of HV test network with different design redundancy options

Figure 14.13 shows the illustration of HV spur supplying one to five (five is shown) distribution transformers and with an option to upgrade to main by adding backfeed connection.

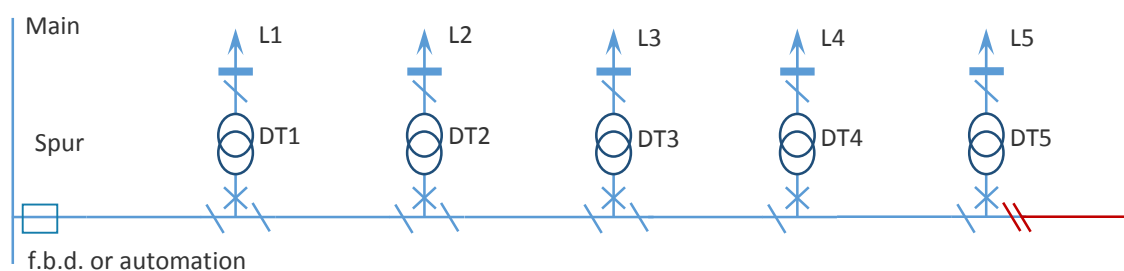


Figure 14.13: Illustration of HV spur with an option to upgrade to main by adding backfeed connection

14.2 Asset Cost

Table 14.2 shows agreed average asset replacement unit cost. Agreed sensitivity range is $\pm 20\%$.

Table 14.2: Average asset replacement unit cost (£k/unit), sensitivity range is $\pm 20\%$

Voltage level	Asset Name	Units	Cost (£k/unit)
132kV	Overhead Line: new trident single circuit line	km	87
	Overhead Line: double circuit tower	km	220
	Overhead Line: restring to upgrade	km	53
	UG Cable (Non Pressurised)	km	1215
	CB (Air Insulated Busbars) (ID&OD) (GM)	Each	500
	CB (Gas Insulated Busbars) (ID) (GM)	Each	900
	Switchgear – Other	Each	45
	Transformer	Each	1100
	EHV	Overhead Line Pole / Tower	km
UG Cable		km	290
CB (Air Insulated Busbars) (ID&OD) (GM)		Each	75
CB (Gas Insulated Busbars) (ID) (GM)		Each	110
RMU		Each	100
Switch (GM)		Each	60
Switch (PM)		Each	10
Switchgear – Other		Each	10
Transformer		Each	400
HV	Overhead Pole Line	km	30
	UG Cable	km	110
	CB (GM) Primary	Each	40
	CB (GM) Secondary	Each	8
	Switch (GM)	Each	8
	RMU	Each	12
	CB (PM)	Each	8
	Switch (PM)	Each	10
	Switchgear – Other (PM)	Each	2.9
LV	Transformer (PM) Low loss	Each	4.3
	Transformer (GM)	Each	15
	Overhead Pole Line	km	19
	UG Cable	km	101
	CB	Each	5
Pillar at Substation	Each	9.5	

	UGB and Pillar – Other	Each	5.5
	Board	Each	18
	Link box	Each	1.5
	Overhead line link	Each	0.75
	Transformer/Regulators	Each	3

Annuity factor for CAPEX is 10.

14.3 Detailed Cable and Substation Costs

Table 14.3 contains agreed detailed cost for a set of cables with different cross sectional area.

Table 14.3: 33 kV cable cost

Cable	Rating (Amps) (direct laying)	Cost (£/km)
33kV 185mm ²	460 – 445	227,390
33kV 240mm ²	530-520	237,130
33kV 400mm ²	690-630	261,910
33kV 500mm ²	760 - 700	283,980

Agreed reinforcement cost of a HV/LV substation:

- Urban: Larger transformer plus new LV board plus jointing ~ £23k
- Rural: Lager PMT plus pillar plus LV network ~ £10k

Primary substation

Table 14.4 and Table 14.5 shows agreed typical cost of primary substations including civils, protection, 11 kV transformer and bus section CBs and 5 km EHV cable per transformer and a spare CB at BSP.

Table 14.4: Typical cost of primary substations including civils, protection, 11 kV transformer and bus section CBs and 5 km EHV cable per transformer and a spare CB at BSP

	Asset	Unit £k	No	subtotal £k	Total £k	
4/8 MVA x 4	4/8 MVA	134	4	536		
	185 cable	237	20	4740		
	Civils, protection				500	
	11kV Tx CB	20	4	80		
	11kV B/S CB	20	3	60	5916	
7.5/15 MVA x 3	7.5/15 MVA	162	3	486		
	185 cable	237	15	3555		
	Civils, protection				500	
	11kV Tx CB	20	3	60		
	11kV B/S CB	20	2	40	4641	
16/32 MVA x 2	16/32 MVA	228	2	456		
	185 cable	237	10	2370		
	Civils, protection				500	

	Asset	Unit £k	No	subtotal £k	Total £k
	11kV Tx CB	2	20	40	
	11kV B/S CB	1	20	20	3386

Table 14.5: Typical cost of primary substations including civils, protection, 11 kV transformer and bus section CBs and 5 km EHV cable per transformer and a spare CB at BSP

Rated voltage (kV)	Rated power (MVA)	Typical cost of substation (£k)
33/11	4x4/8	5,916
	3x7.5/15	4,641
	2x16/32	3,386

To match the same N-1 emergency rating substation cost is adjusted by plotting cost per number of transformers in a substation and finding a linear trendline as shown in Figure 14.14.

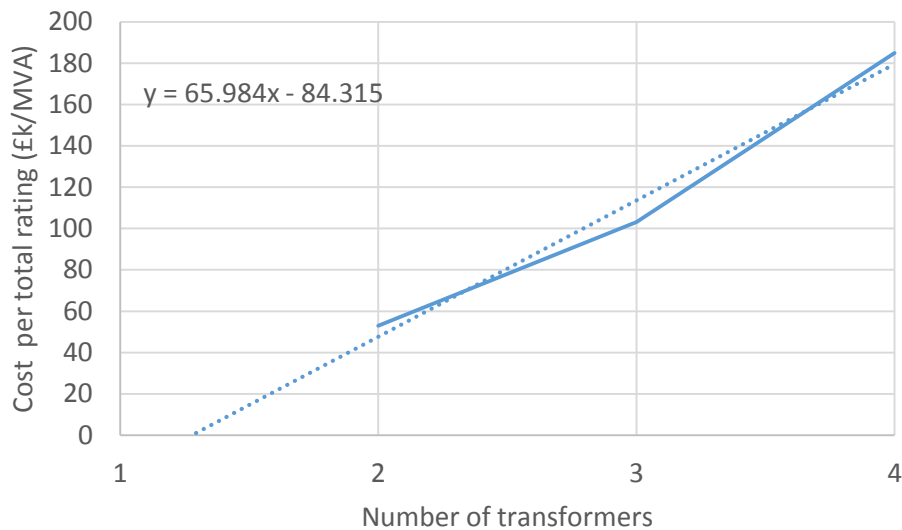


Figure 14.14: Typical cost of primary substation

Linearised typical cost of primary substation including 5 km of cables per transformer is then $(£66k/MVA \times N - £84k/MVA) \times N \times ER$, where N is the number of transformers and ER emergency rating (MVA). Obtained cost is summarised in Table 14.6. In a similar way a cost of substation with one km of transformers' feeder cable is estimated and presented in the Table.

Table 14.6: Substation cost including cost of cables and switchgears but excluding land cost

EHV/HV Substation	Cost (£k/year)	
	Cable 5 km	Cable 1 km
2x30 MVA	285.9	129.9
3x15 MVA	511.4	194.4
4x10 MVA	718.5	259

Bulk supply substation

Table 14.7 and Table 14.8 shows agreed typical cost of BSP substations including civils, protection, 11 kV transformer and bus section CBs and 5 km 132 kV cable per transformer and a spare CB at GSP.

Table 14.7: Typical cost of bulk supply substation assuming 5 km 132 kV cable per transformer and a spare CB at GSP; note ^a assumed cost of transformer

	Asset	Unit £k	No	subtotal £k	Total £k
22.5/45 x 4	22.5/45 MVA	400 ^a	4	1,600	
	300 cable	800	20	16,000	
	Civils, protection			500	
	33kV Tx CB	90	4	360	
	33kV B/S CB	90	3	270	18,730
30/60 x 3	30/60 MVA	500	3	1,500	
	300 cable	800	15	12,000	
	Civils, protection			500	
	33kV Tx CB	90	3	270	
	33kV B/S CB	90	2	180	14,450
45/90 x 2	45/90 MVA	559	2	1,118	
	300 cable	800	10	8,000	
	Civils, protection			500	
	33kV Tx CB	90	2	180	
	33kV B/S CB	90	1	90	9,888

Table 14.8: Typical cost of bulk supply substation assuming 5 km 132 kV cable per transformer and a spare CB at GSP

Rated voltage (kV)	Rated power (MVA)	Typical cost of substation (£k)
132/33	4x22.5/45	18,730
	3x30/60	14,450
	2x45/90	9,888

To match the same N-1 emergency rating bulk supply substation cost is adjusted by plotting cost per MVA against the number of transformers in a substation and finding a linear trendline as shown in Figure 14.15.

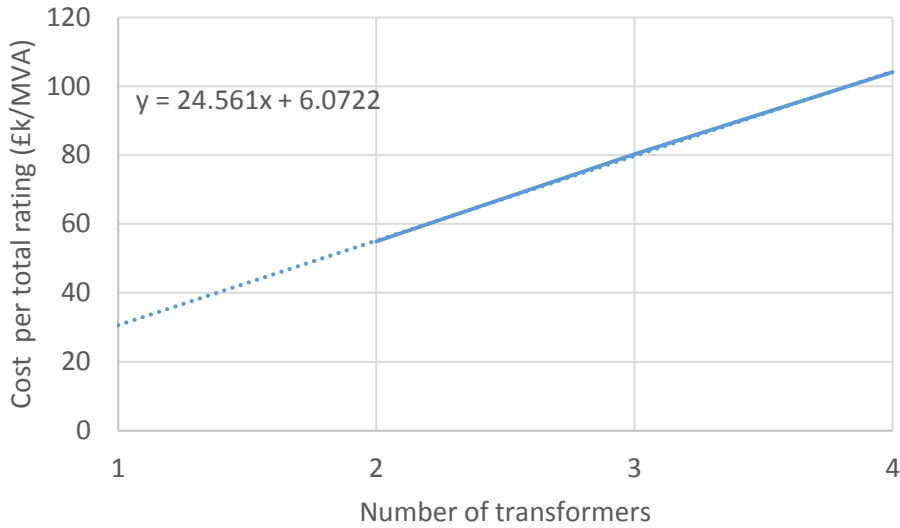


Figure 14.15: Typical cost of bulk supply substation

Linearised typical cost of bulk supply substation including 5 km of cables per transformer is $(£24.6\text{k/MVA} \times N + £6\text{k/MVA}) \times N \times \text{ER}$, where N is the number of transformers and ER emergency rating (MVA). Obtained cost is summarised in Table 14.9. In addition, in the same way substation cost with one km of transformer feeder cable is estimated.

Table 14.9: Substation cost

132kV/EHV Substation	Cost (£k/year)	
	Cable 5 km	Cable 1km
2x90 MVA	993.5	353.5
3x45 MVA	1,076.7	356.7
4x30 MVA	1,251.8	398.5

14.4 Load Duration Curve

Figure 14.16 shows normalised load duration curves with load factors of about 45% and 63%.

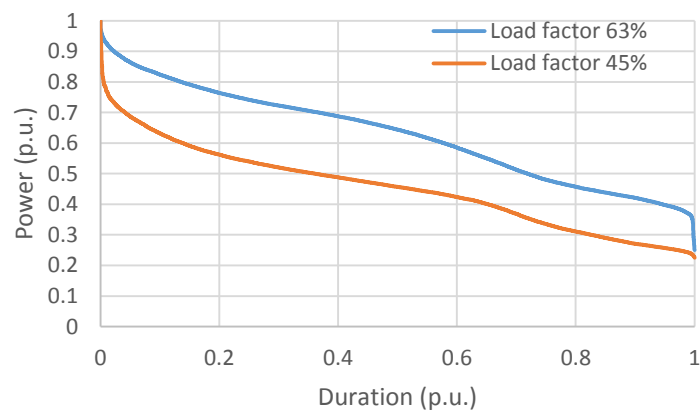


Figure 14.16: Load duration curves with load factors about 45% and 63%

Table 14.10 shows typical range of load factors at different voltage levels.

Table 14.10: Typical range of load factors

Voltage level	Load factor (annual)	Load factor (maintenance window)
LV feeder	20-45%	
HV/LV PMT	30-50%	
HV/LV GMT	40-60%	35-55%
HV	45-65%	40-60%
EHV/HV	50-70%	45-65%
EHV	50-70%	45-65%
132kV/EHV	55-75%	50-70%
132kV	55-80%	50-70%

14.5 Generalised Range of Reliability Related Parameters

Table 14.11 shows agreed range of failure rates, repair times, and upgrade and repair cost.

Table 14.11: Reliability related parameters

Asset	Failure rate (%/unit.year)	Urgent repair time (hours)	Average normal repair time (hours)	Upgrade cost (£k/unit)	Repair cost (£k)
132 kV overhead line (km)	2-15	24	240	87	3.8
132 kV underground cable (km)	2-8	48-120	240	1,215	50
132kV/EHV transformer	1-10	240	720	1,100	1,000
EHV overhead line (km)	2-15	12	120	39-46	3.8
EHV underground cable (km)	2-8	24-72	240	290	19.5
EHV/HV transformer	1-10	192	720	400	250
EHV and HV busbars	0.1	24	240		
HV overhead line (km)	5-8.4-20	6	120	30	2.1
HV underground cable (km)	2-4.8-10	6-18	120	110	8.4
HV/LV PMT transformer	2-20	8-10	24	4.3	4
HV/LV GMT transformer	2-20	24	48	15	7
LV overhead line (km)	10-50	4	4	19	1.1
LV underground cable (km)	10-50	8	8	101	3.3

Note: average normal repair time assumes a half of regular repair time; OH line common mode failure rate sensitivity 0, 5% and 10% of single outage failure rate

Table 14.12 shows agreed transformer feeder maintenance parameters.

Table 14.12: Transformer feeder maintenance parameters

Asset	Typical frequency (%/year)	Emergency return to service time (hours)	Outage time (hours)
132kV/EHV transformer circuit maintenance	12.5%	12	240
EHV/HV transformer circuit maintenance	12.5%	9	120
HV/LV GMT	10%	8	8

Note: depending on the number of operations of OLTC maintenance might be carried out sooner

Table 14.13 shows agreed durations of networks reconfiguration.

Table 14.13: Network reconfiguration duration

Switching	Feeder resupply time (minutes)	Backfeed resupply time (minutes)
Protection	0	0
Automation	3	3
Remote control	10	10
Manual switching	30-60	50

Note: each additional stage of manual switching adds another 20 minutes; remote control of switchgear assumed as available in all primary and bulk supply substations, EHV and 132 kV networks.

List of alternative supply options:

- Resupply with mobile generation within 3-6 hours for HV outages and on average 4.5-10 hours for primary and bulk transformers, EHV, and 132 kV circuits with maximum of 10 MW of units used. Renting cost of 500 kW and below unit is £500-1,750/day while of 1,000 kW unit is £1,000-3,500/day.
- Temporary cable laying within 36 hours at a cost of £50,000-200,000. This option is relevant for outage of EHV/HV and 132kV/EHV, HV transformers and 132kV underground cables.
- Voltage reduction within 3 minutes and each 1% V corresponds to 1.15% MW reduction.

15 GLOSSARY

Term	Description
ACS	Amalgamated Customer Surveys
ANM	Active Network Management
BOCS	Black Out Case Study
BS	British Standard
BSP	Bulk Supply Point
CB	Circuit Breaker
CBA	Cost Benefit Analysis
CDF	Customer Damage Function
CI	Customer Interruption. The number of customers whose supply have been interrupted per 100 customers per year over all incidents, where an interruption of supply lasts for three minutes or longer, excluding reinterruptions to the supply of customers previously interrupted during the same incident.
CMF	Common Mode Failure
CML	Customer Minutes Lost. The average customer minutes lost per customer per year, where an interruption of supply to customer(s) lasts for three minutes or longer.
CPS	Cyber Physical System
CS	Customer Surveys
CVaR	Conditional Value at Risk is a risk assessment technique that could be used to reduce the probability of incurring large loses
DER	Distributed Energy Resources
DG	Distributed Generation. Any generation which is connected to the local distribution network, as well as combined heat and power schemes of any scale.
DLR	Dynamic Line Rating
DNO	Distribution Network Operator
DSR	Demand Side Response
EENS	Expected Energy Not Supplied is the mathematical expectation of the energy which exceeds the available capacity taking into account possible outages
EHV	Extra High Voltage distribution networks with voltage 33 kV and above, including 66 kV networks
ELCC	Effective Load Carrying Capability is the amount of additional incremental load a resource could be expected to serve taking into account probabilistic nature of the electricity supply system
ENS	Energy Not Supplied
EO/C	Economic Output to Energy Consumption
ES	Energy Storage
Failure rate	The number of unplanned failures per unit per year of the specific category of distribution assets
GB	Great Britain
HILP	High Impact Low Probability (HILP) are extreme events that could result in the prolonged loss of supply to localities that have a high gross [economic] value added (GVA). HILP activity relates to increasing the security of supply, to localities that have a high GVA, to levels that exceeds P2/6 recommended levels.
HV	High Voltage distribution networks with voltage 1 kV and above up to but not including 22 kV, including 11 kV and 20 kV
I&C	Industrial and Commercial customers
ICT	Information and Communication Technology

Term	Description
kVA	Kilo Volt Ampere
kWh	Kilo Watt hour
LCNF	Low Carbon Network Fund is a mechanism introduced under the fifth distribution price control review to encourage the DNOs to prepare for the role they would play as GB moves to a low carbon economy...
LTC	Load Transfer Capability
LV	Low Voltage refers to voltages up to, but not including, 1 kV
MCS	Mapped Customer Surveys
Min-Max Regret	An optimisation approach which minimises the maximum of regret cost
MTBF	Mean Time Between Failures
MTTR (repair)	Mean Time To Repair is the average time expressed in hours needed to repair the faulty component in question. In this case, the faulty component has been isolated in order for the repair process to proceed. MTTR abbreviation is shared with Mean Time to Restore but from context it is possible to distinguish between them.
MTTR (restore)	Mean Time To Restore; the average time expressed in hours needed to restore the supply of the customers being interrupted. This process may require urgent short-term repair.
MVA	Mega Volt Ampere
MW	Mega Watt
MWh	Mega Watt hour
N-1	The degree of network redundancy where the system can still supply all loads even if one component of it fails to function.
NOP	Normally Open Point
NPV	Net Present Value is the discounted sum of future cash flows, whether positive or negative, minus any initial investment.
Ofgem	Office of Gas and Electricity Markets
OH	Network dominated with over-head lines
OHL	Over Head Line
P2	A guidance document on system planning and network capacity requirements and details the minimum standards for the security of supply of distribution networks
QB	Quadrature-booster
ROA	Real Options Analysis
SAIDI	System average interruption duration index is the average duration of sustained consumer interruptions per consumer occurring during the analysis period. It is the average time consumers were without power. It is determined by dividing the sum of all sustained consumer interruption durations, in minutes, by the total number of consumers served [167]
SAIFI	System average interruption frequency index The average frequency of sustained interruptions per consumer occurring during the analysis period. It is calculated by dividing the total number of sustained consumer interruptions by the total number of consumers served [167]
SME	Small and Medium-sized Enterprises
SOC	State of Charge of energy storage
SOP	Soft Open Point is power electronic devices installed in place of normally-open points in electrical power distribution network
SPS	Special Protection Scheme
UG	Network dominated with underground cables
UGC	Underground cables

Term	Description
VoLG	Value of Loss Generation is the aggregated or average value of outage costs across distributed generation
VoLL	Value of Loss Load is the aggregated or average value of outage costs across the whole range of consumers in the electricity supply industry [167]. London Economics report estimate it at £17,000/MWh as a load-share weighted average across domestic and SME customers.
VoSL	Value of Shift Load
WTA	Willingness To Accept is an approach to determine how much the consumers are willing to pay to avoid an outage [167]